

1 **Loss of ZnT8 function protects against diabetes by enhanced insulin**
2 **secretion**
3
4 Om Prakash Dwivedi^{1#}, Mikko Lehtovirta^{1#}, Benoit Hastoy^{2#}, Vikash Chandra³, Sandra Kleiner⁴,
5 Deepak Jain⁵, Ann-Marie Richard⁶, Nicola L. Beer², Nicole A. J. Krentz⁷, Rashmi B. Prasad⁸, Ola
6 Hansson^{1,8}, Emma Ahlqvist⁸, Ulrika Krus⁸, Isabella Artner⁸, Daniel Gomez⁴, Aris Baras⁴, Fernando
7 Abaitua⁷, Benoite Champon⁷, Anthony J Payne⁷, Daniela Moralli⁷, Soren K. Thomsen², Philipp
8 Kramer⁷, Ioannis Spiliotis², Reshma Ramracheya², Pauline Chabosseu⁹, Andria Theodoulou⁹,
9 Rebecca Cheung⁹, Martijn van de Bunt^{2,7}, Jason Flannick^{10,11}, Maddalena Trombetta¹², Enzo
10 Bonora¹², Claes B. Wolheim⁸, Leena Sarelin¹³, Riccardo C. Bonadonna¹⁴, Patrik Rorsman², Guy A
11 Rutter⁹, Benjamin Davies⁷, Julia Brosnan⁶, Mark I. McCarthy^{2,7,15}, Timo Otonkoski³, Jens O.
12 Lagerstedt⁵, Jesper Gromada⁴, Anna L. Gloyn^{2,7,15*}, Tiinamaija Tuomi^{1,13,16} and Leif Groop^{1,8*}

13

- 14 1. Institute for Molecular Medicine Finland (FIMM), Helsinki University, Helsinki, Finland.
- 15 2. Oxford Centre for Diabetes Endocrinology & Metabolism, University of Oxford, UK.
- 16 3. Research Programs Unit, Molecular Neurology and Biomedicum Stem Cell Centre, Faculty of Medicine,
17 University of Helsinki, Finland.
- 18 4. Regeneron Pharmaceuticals, Tarrytown, New York, USA.
- 19 5. Department of Experimental Medical Science, Lund University, 221 84, Lund, Sweden.
- 20 6. Pfizer Inc, Cambridge, MA, United States of America.
- 21 7. Wellcome Centre for Human Genetics, University of Oxford, UK.
- 22 8. Lund University Diabetes Centre, Department of Clinical Sciences, Lund University, Skåne University
23 Hospital, SE-20502 Malmö, Sweden.
- 24 9. Section of Cell Biology, Department of Medicine, Imperial College London, Imperial Centre for Translational
25 and Experimental Medicine, Hammersmith, Hospital, Du Cane Road, London, W12 0NN, UK.
- 26 10. Department of Molecular Biology, Massachusetts General Hospital, Boston, Massachusetts, USA.
- 27 11. Program in Medical and Population Genetics, Broad Institute, Cambridge, Massachusetts, USA.

- 28 12. Department of Medicine, University of Verona and Azienda Ospedaliera Universitaria Integrata of Verona,
29 Verona, Italy
- 30 13. Folkhälsan Research Center, Helsinki, Finland.
- 31 14. The Azienda Ospedaliera Universitaria of Parma, 43125 Parma, Italy.
- 32 15. Oxford NIHR Biomedical Research Centre, Churchill Hospital, Oxford, UK
- 33 16. Abdominal Center, Endocrinology, Helsinki University Central Hospital; Research Program for Diabetes and
34 Obesity, University of Helsinki, Helsinki, Finland.

35 # These authors contributed equally to the study

36 *Correspondence: Leif Groop, Institute for Molecular Medicine Finland (FIMM), Helsinki University. Leif.
37 Groop@helsinki.fi and/or leif.Groop@med.lu.se and Anna L Gloyn, Oxford Centre for Diabetes Endocrinology &
38 Metabolism, University of Oxford, UK. anna.gloyn@drl.ox.ac.uk

39

40

41

42

43

44

45

46

47

48

49

50

51

52

53

54

55

56

57

58

59

60

61

62

63

64

65

66

67

68

69 **Abstract**

70 A rare loss-of-function variant p.Arg138* in *SLC30A8* encoding the zinc transporter 8 (ZnT8)
71 enriched in Western Finland protects against type 2 diabetes (T2D). We recruited relatives of the
72 identified carriers and showed that protection was associated with better insulin secretion due to
73 enhanced glucose responsiveness and proinsulin conversion, especially compared with individuals
74 matched for the genotype of a common T2D risk variant in *SLC30A8*, p.Arg325. In genome-edited
75 human IPS-derived β -like cells, we establish that the p.Arg138* variant results in reduced *SLC30A8*
76 expression due to haploinsufficiency. In human β -cells loss of *SLC30A8* leads to increased glucose
77 responsiveness and reduced K_{ATP} channel function, which was also seen in isolated islets from
78 carriers of the T2D-protective allele p.Trp325. These data position ZnT8 as an appealing target for
79 treatment aiming at maintaining insulin secretion capacity in T2D.

80

81 **Introduction**

82 Zinc transporters (ZnTs) regulate the passage of zinc across biological membranes out of the
83 cytosol, while Zrt/Irt-like proteins transport zinc into the cytosol¹. ZnT8, encoded by *SLC30A8*, is
84 highly expressed in membranes of insulin granules in pancreatic β -cells, where it transports zinc
85 ions for crystallization and storage of insulin². We have described a loss-of-Function (LoF) variant
86 p.Arg138* (rs200185429, c.412C>T) in the *SLC30A8* gene, which conferred 53% protection
87 against T2D³. This variant was extremely rare (0.02%) in most European countries but more
88 common (>0.2%) in Western Finland³. We also reported a protective frameshift variant
89 p.Lys34Serfs*50 conferring 83% protection against T2D in Iceland. A recent (>44K) exome
90 sequencing study reported >30 alleles in *SLC30A8* reducing the risk of T2D, confirming it as a
91 robust target for T2D protection⁴. Further, the *SLC30A8* gene also harbors a common variant
92 (rs13266634, c.973T>A) p.Trp325Arg in the C-terminal domain⁵. While the major p.Arg325 allele
93 (>70% of the population) confers increased risk for T2D, the minor p.Trp325 allele is protective⁶.

94 The mechanisms by which reduced activity of ZnT8 protect against T2D are largely unknown.
95 Several attempts have been made to study loss of *Slc30a8* function in rodent models, but the results
96 have been inconclusive: knock-out of *Slc30a8* led to either glucose intolerance or had no effect in
97 mice^{7,8,9}, while over-expression improved glucose tolerance without effect on insulin secretion¹⁰. In
98 a mouse model harbouring the equivalent of the human p.Arg138* variant we were unable to detect
99 any ZnT8 protein and observed no effect on glucose¹¹. These rodent *in vitro* and *in vivo* experiments
100 present a complex picture which might not recapitulate the T2D protective effects by *SLC30A8* LoF
101 mutations in humans. We therefore performed detailed metabolic studies in human carriers of the
102 LoF variant (p.Arg138*) recruited on the basis of their genotype, performed comprehensive
103 functional studies in human β -cell models and compared with the mouse model carrying the human
104 p.Arg138*-*SLC30A8* mutation.

105

106

107 **Results**

108 **Recruitment by genotype**

109 Given the enrichment of the p.Arg138*-*SLC30A8* variant in Western Finland, we genotyped
110 >14,000 individuals from the Botnia Study¹² for the *SLC30A8* p.Arg138* mutation and the common
111 p.Trp325Arg variant (Fig. 1). None of the p.Arg138* mutation carriers was homozygous for the
112 protective common variant, p.Trp325 and p.Arg138* segregated with p.Arg325 in the families
113 (Supplementary Fig. 1). Thus, we present the data in three different ways: 1) p.Arg138* vs. all
114 p.Arg138Arg, 2) p.Arg138* vs. p.Arg138Arg having at least one p.Arg325 allele (p.Trp325Arg or
115 p.Arg325Arg), and 3) p.Arg325 (p.Trp325Arg or p.Arg325Arg) vs. p.Trp325Trp on a background
116 of p.Arg138Arg. We included 79 p.Arg138* carriers and 103 non-carriers. Of them, 54 p.Arg138*
117 and their 47 relatives with p.Arg138Arg participated in a test meal (Fig. 1 and Supplementary Table
118 1). In addition, 35 p.Arg138* and 8141 p.Arg138Arg had previously undergone an oral glucose
119 tolerance test (OGTT, Fig. 1 and Supplementary Table 2).

120 Replicating our previous findings³, carriers of p.Arg138* had reduced risk of T2D (OR=0.40,
121 P=0.003) in analysis of total 4564 T2D subjects (13 p.Arg138* carriers) and 8183 non-diabetic (55
122 p.Arg138* carriers) individuals. Additionally, non-diabetic p.Arg138* carriers have lower fasting
123 glucose concentrations (P=0.033) than p.Arg138Arg. There were no significant differences in
124 plasma zinc concentrations measured during test meal or OGTT (data not shown).

125 *Comparison of p.Arg138* vs. p.Arg138Arg*: The p.Arg138* carriers have lower blood glucose
126 levels during test meal specifically during the first 40 minutes (P=0.02) and better corrected insulin
127 response (CIR) (at 20 min, p=0.046) than non-carriers (Fig. 2a and Supplementary Tables 3).
128 Similarly, the carriers had better insulin response to OGTT (Fig 3b-c, left panel), especially the
129 early incremental insulin response (p=0.008) and insulin/glucose ratio (at 30 min, p=0.002,

130 Supplementary Tables 4). Of note, the p.Arg138* carriers had significantly lower proinsulin/C-
131 peptide (20 min: P=0.041; 40 min: P=0.043) and proinsulin/insulin (20 min: P=0.006) ratios during
132 test meal suggesting effects on proinsulin conversion (Fig. 2d-e). No differences were seen in
133 glucagon, GLP-1 or free fatty acids concentrations during test meal (Supplementary Fig. 2c-e).
134 Neither model-based insulin clearance index nor the ratio of insulin and C-peptide areas under the
135 curve during test meal differed between p.Arg138* and p.Arg138Arg, making changes in insulin
136 clearance¹³ unlikely (Supplementary Fig. 2f-g).

137 *Comparison of p.Arg138* vs. p.Arg138Arg-p.Arg325:* The above differences were magnified when
138 we restricted the p.Arg138Arg group to carriers of the common risk variant p.Arg325 (middle panel
139 of Fig. 2). The early phase (0-40 min) insulin (p=0.026), insulin/glucose ratio (p=0.004) and CIR
140 (p=0.004; 20 min, Supplementary Table 3) were all greater in p.Arg138* carriers compared with
141 those having p.Arg138Arg on a background of p.Arg325. Both the proinsulin/C-peptide (20 min:
142 P=0.027, 40 min: P=0.044) and proinsulin/insulin ratios (20 min: P=0.003) were reduced in
143 p.Arg138* carriers (middle panel of Fig. 2d-e).

144 *Comparison of p.Trp325Trp vs. p.Arg325:* The effect of p.Trp325Trp genotype on glucose and
145 insulin response mimicked the effects of p.Arg138* with pronounced early (20 min) insulin
146 (p=0.035) and C-peptide (p=0.025) responses during test meal (right panel of Fig. 2b-c and
147 Supplementary Fig. 2a), as well as increased insulin secretion (30 min insulin, 30 min
148 insulin/glucose, incremental insulin, $P \leq 0.003$) and lower fasting and 120 minute proinsulin
149 (p=0.006 and p=0.039, respectively) concentration during OGTT in p.Trp325 carriers
150 (Supplementary Table 4, right panel of Fig. 3b-c). Moreover, p.Trp325Trp carriers undergoing
151 intravenous glucose tolerance tests (IVGTT) showed a pronounced (p=0.003) early incremental
152 insulin secretion response (Supplementary Fig. 3a-b and Supplementary Table 4). In patients with
153 newly diagnosed T2D, the p.Trp325Trp carriers showed a trend (P=0.12) to enhanced β -cell
154 sensitivity to glucose during the OGTT (Supplementary Fig. 3c).

155 Taken together, all the human *in vivo* results show that T2D protection by the LoF variant
156 p.Arg138* is due to enhanced glucose-stimulated insulin secretion combined with enhanced
157 proinsulin conversion. The common T2D protective allele p.Trp325 shows a similar – albeit weaker
158 - metabolic phenotype suggesting it might also reduce ZnT8 function.

159 ***SLC30A8* p.Arg138* variant in human iPSCs**

160 The majority of nonsense *SLC30A8* alleles (including p.Arg138*) protecting against T2D are
161 located in the first four exons of the eight-exon canonical islet *SLC30A8* transcript
162 ENST00000456015 and are predicted to undergo nonsense mediated decay (NMD), a cell
163 surveillance pathway which reduces errors in gene expression by eliminating mRNA transcripts that
164 contain premature stop codons. To confirm that the p.Arg138* allele indeed leads to
165 haploinsufficiency through NMD, we used CRISPR-Cas9 to introduce the p.Arg138* variant into
166 the *SLC30A8* locus of the SB Ad3.1 human iPSC cell line (Supplementary Fig. 4a, Methods). Two
167 hiPSC lines for the p.Arg138*-*SLC30A8* variant (Clone B1 and A3) were generated and compared
168 to an unedited p.Arg138Arg-*SLC30A8* CRISPR hiPSC line. Both B1 and A3 clones were
169 heterozygous with mono-allelic sequencing confirming the p.Arg138* variant in only one allele
170 (Supplementary Fig. 4b). All hiPSC lines passed quality control checks including karyotyping and
171 pluripotency (Supplementary Fig. 4c).

172 Accordingly, we subjected our *SLC30A8*-edited iPSCs to a previously published *in vitro* endocrine
173 pancreas differentiation protocol¹⁴ (Supplementary Fig. 4d-k, Methods). At the end of the seven
174 stage protocol, *SLC30A8* expression was significantly reduced in cells heterozygous for the
175 p.Arg138* allele (clone B1 0.09±0.04; clone A3 0.08±0.05) compared to unedited control cells
176 (1.03±0.11) (Fig. 4a). Of note, p.Arg138* allele specific *SLC30A8* expression was reduced
177 compared to the WT allele¹⁵ (clone B1: 22.9±2.1%; clone A3: 26.0±3.9%) (Fig. 4b-c). Inhibition of
178 NMD by cyclohexamide increased expression of the p.Arg138* transcript more than the
179 p.Arg138Arg transcript compared to DMSO control (clone B1: 209±52% and clone A3: 199±67%

180 vs. clone B1: $161 \pm 30\%$ and clone A3: $132 \pm 35\%$, respectively, Fig. 4d-e). Taken together, these data
181 show that the protective p.Arg138*-*SLC30A8* allele undergoes NMD, resulting in
182 haploinsufficiency for *SLC30A8*.

183 **Impact of *SLC30A8* loss in a human β -cell line**

184 Since human *in vivo* studies provided strong evidence for a role of the p.Arg138* on insulin
185 secretion and proinsulin processing, we studied the impact of *SLC30A8* loss using siRNA mediated
186 knock down (KD) on both phenotypes in a well characterized human β -cell model EndoC- β H1¹⁶
187 (Methods). By siRNA, we achieved 55-65% decrease in *SLC30A8* mRNA ($p=0.008$) and protein
188 ($p=0.016$, Fig. 5a-c).

189 KD of *SLC30A8* had no significant effect on glucose- or tolbutamide-stimulated insulin secretion or
190 on insulin content (Fig. 5d-e) but basal insulin secretion was higher in si*SLC30A8* transfected cells
191 compared to scrambled siRNA cells ($p=0.012$, Fig. 5d), and the inhibitory effect of diazoxide, a
192 K_{ATP} channel opener, on glucose-stimulated insulin secretion was reduced ($p=2 \times 10^{-3}$, Fig. 5d). We
193 measured the resting membrane conductance (G_m), which principally reflects K_{ATP} channel activity.
194 In control cells, G_m was in agreement with that previously reported¹⁷. *SLC30A8* KD reduced G_m by
195 65% ($p=0.002$, Fig. 5f) without effect on cell size (Fig. 5g), an effect that correlated with reduced
196 expression of the two genes encoding the K_{ATP} channel subunits SUR1 (*ABCC8*) and Kir6.2
197 (*KCNJ11*) (Fig. 5h). However, insulin secretion elicited by increasing extracellular K^+ ($[K^+]_o$) to 50
198 mM (to depolarise the cells and open voltage-gated Ca^{2+} channels) and 16.7 mM glucose was
199 significantly higher after *SLC30A8* KD ($p=0.008$, Fig. 5i). The proinsulin-insulin ratios (both total
200 and secreted hormones) were decreased in si*SLC30A8* cells ($p<0.001$, Fig. 5j-k). Although mRNA
201 of the proinsulin processing genes *PC1/3* and *CPE* was decreased, we could not detect a similar
202 reduction at the protein level (Fig. 5l-n).

203 RNA sequencing of *SLC30A8* KD cells (n=3 vs. 3) replicated the reduction of *KCNJ11* and *ABCC8*
204 gene expression ($p=4.3 \times 10^{-3}$ and $p=2.9 \times 10^{-5}$, respectively). In addition, expression of genes
205 involved in regulation of β -cell excitability was down-regulated, including *KCNMA1* encoding a
206 Ca^{2+} -activated K^{+} channel¹⁸ and *TMTC1* ($p=6.8 \times 10^{-5}$ and 2.9×10^{-16} , respectively) encoding an ER
207 adapter protein influencing intracellular calcium levels. Also, expression of genes associated with
208 β -cell maturation and secretion was influenced by *SLC30A8* KD with decreased expression of
209 *NKX6.1* and *PDX1* and increased expression of *SOX4*, *SOX6* and *SOX11* (Fig. 5o-p).
210 In addition, we also observed increased AKT phosphorylation (pAKT-473) and improved cell
211 survival under ER stress ($p<0.017$, Fig. 5q-s), mechanisms which also could contribute to the
212 overall protection by preserving β -cell mass¹⁹. Taken together, these data generated by disrupting
213 *SLC30A8* in a human β -cell pointed at multiple mechanisms including changes in proinsulin
214 conversion, K_{ATP} channel activity and cell viability.

215 **Metabolic phenotype of mice carrying the human *SLC30A8* p.Arg138***

216 Since neither global nor tissue specific *Slc30a8* KD mouse models have recapitulated the human
217 phenotype in carriers of the *SLC30A8* p.Arg138* variant, we tried to overcome this problem by
218 using a mouse model carrying the *Slc30a8* p.Arg138* variant¹¹. These mice do not express the
219 truncated ZnT8 protein¹¹. On a standard chow diet there was no evidence for enhanced insulin
220 secretion¹¹. However, we examined whether they might do so on a high fat diet (HFD). This was
221 indeed the case (Fig. 6a-h), and the same differences in proinsulin/insulin and proinsulin/C-peptide
222 ratios were seen as in humans. No changes were seen in insulin clearance.

223 **Impact of p.Arg138* on protein localization and cytosolic zinc distribution in INS-1 cells**

224 Although we found no evidence in either mouse or our human β -cell model to support the presence
225 of a truncated protein we explored the possibility of what might happen if a truncated protein
226 resulted from mRNA evading NMD. Transient overexpression of tagged ZnT8-p.Arg138* fusion

227 proteins in a rat insulinoma cell line, INS-1e, showed distinct punctate distribution patterns,
228 consistent with localization of the truncated ZnT8 protein to secretory granules, as previously
229 observed with the full length protein²⁰ (Supplementary Fig. 5a-c) Additionally, Western blot
230 showed stable expression of truncated ZnT8 in native INS1e cells (Supplementary Fig. 5d).

231 To investigate the effects of a truncated ZnT8 protein on cytosolic free Zn²⁺, we used a genetically-
232 encoded Zn²⁺ sensor eCALWY-4²¹. Overexpression of the truncated protein (p.Arg138*) had no
233 impact on cytosolic free Zn²⁺ when expressed in INS-1 WT cells ruling out a dominant negative
234 effect for the truncated protein (Supplementary Fig. 5e-h).

235 **Influence of common *SLC30A8* variants p.Trp325Arg in primary human islets**

236 While adult human islets show high levels of *SLC30A8* expression there was no reproducible effect
237 of the p.Arg325Trp variant on *SLC30A8* expression in human islets from cadaveric donors (Fig.
238 7a). Islets obtained from cadaveric p.Trp325 carriers secreted more insulin than p.Arg325Arg
239 carriers (Fig. 7b-e). The increased glucose responsiveness was observed at submaximal glucose
240 stimulation (6 mM) rather than at maximal glucose stimulation (16.7 mM) (Fig. 7b-c). Increasing
241 glucose from 1 mM to 6 mM stimulated insulin secretion 2.2- and 2.7-fold in p.Arg325 and
242 p.Trp325 carriers respectively, with no effect on insulin content (Fig. 7c-d). This secretion pattern
243 echoes the one observed after siRNA of *SLC30A8* KD in EndoC-βH1. Insulin secretion in p.Trp325
244 carriers was also increased at high glucose (16.7 mM) when co-exposed to depolarizing [K⁺]_o (70
245 mM) (Fig. 7e) as also seen after *SLC30A8* KD in EndoC-βH1.

246 As *SLC30A8* is highly expressed in human alpha cells¹, we also measured glucagon secretion from
247 the same islets (Fig. 7f). In islets from p.Arg325Arg donors, 6 mM glucose inhibited glucagon
248 secretion by ~50% compared to 1 mM glucose. In islets from p.Trp325Arg donors, glucagon
249 secretion at 1 mM glucose was reduced by 50% compared to p.Arg325Arg donors with no effect on
250 glucagon content (Fig. 7f-g).

251 We also explored whether the p.Trp325Arg variant would have trans-eQTL effects on genes
252 involved in insulin production and secretion²² (Fig. 7a). Expression of *PCSK1* (P=0.041)
253 and *PCSK2* (P=0.045) were reduced. Among the genes encoding for K_{ATP} channels subunits
254 only *ABCC8* (P=0.049) expression was significantly affected in islets from p.Trp325 carriers
255 compared to non-carriers (Fig. 7a). Taken together, the data suggest the common T2D-protective
256 allele (p.Trp325) may improve the response to a glucose challenge by enhancing insulin secretion
257 and possibly by reducing glucagon secretion in primary human islets.

258 Discussion

259 The current study demonstrates the strengths of using human models for studying the consequences
260 of LoF mutations in humans, particularly by demonstrating a stronger protective effect of
261 p.Arg138* in individuals carrying the common risk p.Arg325 allele on the same haplotype.
262 However, the minor p.Trp325 allele was also associated with protection against T2D albeit less
263 pronounced. This emphasizes the importance of taking into account the genetic background of the
264 human LoF carrier.

265 Whilst the data from all our sub-studies are consistent with increased glucose responsiveness, the
266 precise molecular mechanisms for these phenotypes, involvement of zinc and an explanation for
267 why there are discrepancies between humans and rodents remain elusive. In the IPS-derived beta-
268 like cells, the p.Arg138* variant dramatically lowered expression with evidence of NMD resulting
269 in haploinsufficiency. Similarly, in the mouse model we were unable to detect the truncated
270 protein, but we could detect appreciable levels of RNA¹¹.

271 The most reproducible finding in all sub-studies of p.Arg138* was enhanced glucose-stimulated
272 insulin secretion accompanied by increased conversion of proinsulin to C-peptide and insulin.
273 Carriers of p.Trp325 displayed a similar phenotype, which is in line with a previous study showing
274 impaired proinsulin conversion in carriers of the risk p.Arg325 allele²³. There could also be other

275 potential explanations for this effect, as it has been suggested that it takes some time for insulin to
276 mature and become biologically active^{24,25}. It is possible that the pronounced effects of the LoF
277 mutation at 20 and 40 min of test meal could reflect such a mechanism.

278 The present and previous studies demonstrate that loss of ZnT8 function after silencing the murine
279 gene reduces total cellular zinc content as well as free Zn²⁺ in the cytosol and granules^{7,10,20,26}. LoF
280 p.Arg138* (assuming no or minimal escape from NMD) is therefore likely to exert the same effects
281 on intracellular zinc concentrations and may thus impact insulin secretion through intracellular
282 mechanisms, including potential differences in Zn²⁺ secretion. Also, a recent study showed that the
283 p.Arg325Arg variant was associated with higher islet zinc concentrations²⁷. In the present study
284 over-expression of the LoF mutation p.Arg138* in INS-1 cells did not result in changes in cytosolic
285 zinc concentrations leaving a reduction of zinc in insulin granules as a plausible explanation which
286 still needs to be experimentally confirmed.

287 In support of a protective effect of lowering intracellular zinc concentrations on development of
288 diabetes, in the CNS, Zn²⁺ plays an important role as a regulator of cellular excitability²⁸ and Zn²⁺
289 has been reported to activate K_{ATP} channels²⁹, inhibit L-type voltage-gated Ca²⁺ channels and inhibit
290 insulin secretion³⁰.

291 Taken together, our data consistently demonstrate that heterozygosity for a LoF mutation
292 p.Arg138* and homozygosity for a common variant p.Trp325Trp of the *SLC30A8* are associated
293 with increased insulin secretion capacity and lower risk of T2D without any negative effect.

294 Therefore, ZnT8 remains an appealing safe target for antidiabetic therapy preserving β-cell
295 function.

296

297

298

299 **Methods**

300 **Human study population**

301 The Botnia Study has been recruiting patients with T2D and their family members in the area of
302 five primary health care centers in western Finland since 1990. Individuals without diabetes at
303 baseline (relatives or spouses of patients with T2D) have been invited for follow-up examinations
304 every 3-5 years¹². The Prevalence, Prediction and Prevention of diabetes (PPP)–Botnia Study is a
305 population-based study in the same region including a random sample of 5,208 individuals aged 18
306 to 75 years from the population registry³¹. Diabetes Registry Vaasa (DIREVA) is regional diabetes
307 registry of > 5000 diabetic patients from Western Finland (Botnia region)³². In the current study, we
308 included >14,000 individuals (Botnia family study=5678, PPP=4862, and DIREVA=3835). All
309 participants gave their written informed consent and the study protocol was approved by the Ethics
310 Committee of Helsinki University Hospital, Finland (the Botnia studies) and the Ethics Committee
311 of Turku University Hospital (DIREVA).

312 ***Oral Glucose Tolerance Test (OGTT) and test meal:*** Subjects maintained a weight-maintaining
313 diet and avoided vigorous exercise for 3 days prior to the OGTT or test meal, which were
314 performed after an overnight fast. Height, weight, hip and waist circumferences, fat percentage (%
315 bioimpedance analyzer) and blood pressure (sitting, 3 measurements after 5 min rest) were
316 measured. The participants ingested 75 g dextrose (in a couple of minutes, OGTT) or a 526 kcal
317 mixed meal (in 10 minutes, test-meal: 76 g carbohydrate, 17 g protein and 15 g fat). Blood samples
318 were drawn from an antecubital vein for plasma (P-) glucose and serum (S-) insulin and C-peptide
319 at 0, 30, 120 min during the OGTT; for P-glucose, P-glucagon, S- insulin, S-C-peptide, S-zinc, and
320 total S-GLP-1 at 0, 20, 40, 70, 100, 130, 160 and 190 min during the test meal. Test meal samples
321 for S-FFA were collected at 0, 40 and 120 min and for S-proinsulin at 0, 20, 40 and 130 min,
322 respectively. Urine was collected between 0 – 70 and 70 – 190 min for the determination of glucose
323 and zinc excretion during the test meal.

324 ***Intravenous Glucose Tolerance Test (IVGTT):*** IVGTT group consists of total 849 (male- 403,
325 female- 446) individuals with an average age of 51 years. An antecubital polyethylene catheter was
326 placed to one hand for the infusion of 0.3 g/kg body weight of glucose (maximum dose 35 g)
327 intravenously for 2 min. A retrogradely positioned wrist vein catheter was placed in the other hand,
328 held in a heated (70°C) box in order to arterialize the venous blood. Arterialized blood samples
329 were drawn at 0, 2, 4, 6, 8,10, 20, 30, 40, 50 and 60 min for P-glucose and S-insulin.

330 ***Biochemical measurements:*** P-glucose was analyzed using glucose oxidase (Beckman Glucose
331 Analyzer, Beckman Instruments, Fullerton, CA, USA; Botnia Family Study) or glucose
332 dehydrogenase method (Hemocue, Angelholm, Sweden; PPP-Botnia and test meal studies). In the
333 Botnia Family study, S-insulin was measured by radioimmunoassay (RIA, Linco; Pharmacia,
334 Uppsala, Sweden), enzyme immunoassay (EIA; DAKO, Cambridgeshire, U.K.) or
335 fluoroimmunoassay (FIA, AutoDelfia; Perkin Elmer Finland, Turku, Finland). For the
336 analysis, insulin concentrations obtained with different assays were transformed to cohere with
337 those obtained using the EIA. The correlation coefficient between RIA and EIA as well as between
338 FIA and EIA was 0.98 ($P < 0.0001$). S-insulin was measured by the FIA in baseline visit of PPP-
339 Botnia and the test meal study (correlation co-efficient 0.98). S-proinsulin was measured using RIA
340 (Linco; Pharmacia, Uppsala, Sweden, OGTT data) or EIA (Mercodia AB, Uppsala, Sweden; test-
341 meal data), and P-glucagon using RIA (EMD Millipore, St. Charles, MO; OGTT data) or EIA
342 (Mercodia AB, Uppsala, Sweden; test-meal data). S-FFA was measured by an enzymatic
343 colorimetric method (Wako Chemicals, Neuss, Germany). Serum total cholesterol, HDL and
344 triglyceride concentrations were measured with Cobas Mira analyzer (Hoffman LaRoche, Basel,
345 Switzerland), and since 2006 with an enzymatic method (Konelab 60i analyser; Thermo Electron
346 Oy, Vantaa, Finland). Serum LDL cholesterol was calculated using the Friedewald formula. Blood
347 collected in tubes containing DPP4-inhibitors was used for radioimmunoassay³³ for total P-GLP-1
348 (intact GLP-1 and the metabolite GLP-1 9-36 amide) during test meal.

349 Serum and urine samples for zinc were collected in trace element tubes (Beckton Dickinson, NJ,
350 USA) and S- and U-zinc analyzed by two commercial laboratories: NordLab (Oulu, Finland; atom
351 absorption spectrophotometry, AAS) until 6th May 2015, then in Synlab (Helsinki, Finland; AAS
352 for serum, mass spectrophotometry ICP-MS for U-zinc). The S-zinc concentrations were corrected
353 for P-albumin ($r = 0.34$, $p = 0.008$ Nordlab, $r = 0.34$, $p = 0.03$ Synlab).

354 Corrected insulin response (CIR) was calculated for test meal (at 20 min) and OGTT (at 30 min.)
355 using the formula $CIR(t) = Ins(t) / [Gluc(t) \cdot (Gluc(t) - 3.89)]$, where $Ins(t)$ and $Gluc(t)$ are insulin (in
356 mU/L) and glucose concentrations (in mmol/L) at sample time point t (min)³⁴. Estimation of Insulin
357 clearance index was done on the model based estimation of glucose-, insulin- and C-peptide curves
358 during the test meal using the equation $AUC(ISR) / [(AUC(Ins) + (I(basal) - I(final)) \cdot MRT(Ins))]$,
359 where $AUC(ISR)$ is the area under the curve of insulin secretion rate, $AUC(Ins)$ is the area under
360 the curve of insulin concentration, $I(final)$ is insulin concentration at the end, and $I(basal)$ insulin
361 concentration at the beginning of the study³⁵. $MRT(Ins)$ is the mean residence time of insulin, and
362 was assumed to be 27 minutes as reported previously³⁶.

363 **Genotyping:** We analyzed genotype data for rs13266634 (p.Trp325Arg) and rs200185429
364 (p.Arg138*) for three cohorts genotyped with different genome-/exome-wide chips: the Botnia
365 family cohort (Illumina Global Screening array-24v1, genotyped at Regeneron Pharmaceuticals),
366 PPP-Botnia (Illumina HumanExome v1.1 array, genotyped at Broad Institute³) and DIREVA
367 (Illumina Human CoreExome array-24v1, genotyped at LUDC). For the Botnia family cohort,
368 genotype data for p.Arg138* were imputed (info score >0.95) from the available GWAS data by
369 phasing using SHAPT-IT v2³⁷ and imputing using the GoT2D reference panel³⁸ by IMPUTEv2³⁹.
370 The carrier status of imputed p.Arg138* was additionally confirmed from exome sequencing data.
371 Genotyping (p.Trp325Arg and p.Arg138*) the family members participating in the genotype based
372 recall study (test meal study) was performed using TaqMan (Applied Biosystems, Carlsbad, CA).
373 The genotype distribution of both variants was in accordance with Hardy-Weinberg equilibrium in

374 all the cohorts. We did not detect any Mendelian errors in the families.

375 **Genetic Association Analysis:** All the quantitative traits were inversely normally transformed
376 before the analyses. The family-based recall study included only non-diabetic subjects during test
377 meal and analysis of data was performed using family-based association analyses adjusting for age,
378 sex, BMI, and other covariates if appropriate, using QTDT (v2.6.1)⁴⁰. The significance levels were
379 derived from 100,000 permutations as implemented in QTDT. Also, the OGTT study included only
380 non-diabetic subjects. The association analysis was performed using mixed linear model
381 considering genetic relatedness among samples as implemented in GCTA (v1.91)⁴¹.

382 **Study participants and their clinical measurements in Verona Newly Diagnosed Diabetes Study**
383 **(VNDS):** The Verona Newly Diagnosed Type 2 Diabetes Study (VNDS; NCT01526720) is an
384 ongoing study aiming at building a biobank of patients with newly diagnosed (within the last six
385 months) type 2 diabetes. Patients are drug-naïve or, if already treated with antidiabetic drugs,
386 undergo a treatment washout of at least one week before metabolic tests are performed⁴². Each
387 subject gave informed written consent before participating in the research, which was approved by
388 the Human Investigation Committee of the Verona City Hospital. Metabolic tests were carried out
389 on two separate days in random order⁴². Plasma glucose concentration was measured in duplicate
390 with a Beckman Glucose Analyzer II (Beckman Instruments, Fullerton, CA, USA) or an YSI 2300
391 Stat Plus Glucose&Lactate Analyzer (YSI Inc., Yellow Springs, OH, USA) at bedside. Serum C-
392 peptide and insulin concentrations were measured by chemiluminescence as previously described⁴².
393 The analysis of the glucose and C-peptide curves during the OGTT was carried out with a
394 mathematical model as described previously⁴². This model was implemented in the SAAM 1.2
395 software (SAAM Institute, Seattle, WA) to estimate its unknown parameters. Numerical values of
396 the unknown parameters were estimated by using nonlinear least squares. Weights were chosen
397 optimally, i.e., equal to the inverse of the variance of the measurement errors, which were assumed
398 to be additive, uncorrelated, with zero mean, and a coefficient of variation (CV) of 6-8%. A good fit

399 of the model to data was obtained in all cases and unknown parameters were estimated with good
400 precision. In this paper we report the response of the beta cell to glucose concentration
401 (proportional control of beta cell function), which in these patients accounts for $93.2 \pm 0.3\%$ of the
402 insulin secreted by the beta cell in response to the oral glucose load. Genotypes were assessed by
403 the high-throughput genotyping Veracode technique (Illumina Inc, CA), applying the GoldenGate
404 Genotyping Assay according to manufacturer's instructions. Hardy-Weinberg equilibrium was
405 tested by chi-square test. Variant association analyses were carried out by generalized linear models
406 (GLM) as implemented in SPSS 25.0 and they were adjusted for a number of potential confounders,
407 including age, sex and BMI.

408 **iPSC generation, differentiation and genome editing**

409 ***iPSC generation and maintenance:*** The human induced pluripotent stem cell line (hiPSC) SB
410 Ad3.1 was previously generated and obtained through the IMI/EU sponsored StemBANCC
411 consortium via the Human Biomaterials Resource Centre, University of Birmingham
412 (<http://www.birmingham.ac.uk/facilities/hbrc>). Human skin fibroblasts were obtained from a
413 commercial source (Lonza CC-2511, tissue acquisition number 23447). They had been collected
414 from a Caucasian donor with no reported diabetes with fully informed consent and with ethical
415 approval from the National Research Ethics Service South Central Hampshire research ethics
416 committee (REC 13/SC/0179). The fibroblasts were reprogrammed to pluripotency as previously
417 described⁴³ and were subjected to the following quality control checks: SNP-array testing via
418 Human CytoSNP-12v2.1 beadchip (Illumina #WG-320-2101), DAPI-stained metaphase counting
419 and mFISH, flow cytometry for pluripotency markers (BD Biosciences #560589 and 560126), and
420 mycoplasma testing (Lonza #LT07-118).

421 ***CRISPR-Cas9 mediated generation of p.Arg138* human induced pluripotent stem cell line:***

422 Several guide RNAs (gRNAs) were designed using MIT CRISPR tool (<http://crispr.mit.edu/>) to
423 target near exon 3 of *SLC30A8* (ENST00000456015). The gRNAs were also subjected to an

424 additional BlastN search (www.ensembl.org) to confirm specificity and identified no additional off-
425 target sites. The gRNA (AGCAGGTACGGTTCATAGAG) was sub-cloned into the *BsbI* restriction
426 sites in pX330⁴⁴ plasmid that was previously modified to contain a puromycin selection cassette.
427 Single strand oligonucleotides for homology-directed repair (HDR) were synthesised by
428 Eurogentec, stabilised by addition of a phosphorothioate linkage at the 5' end, and contained two
429 nucleotide changes: i) the T2D-protective nonsense mutation at codon-138 (c.412C>T, p.Arg138*),
430 which also mutated the PAM sequence, and ii) a silent missense mutation at codon-139 (c.417A>T,
431 p.Ala139Ala) to introduce an *AluI* restriction site for genotyping.

432 Human iPSCs were co-transfected with *SLC30A8*-px330-puromycin resistant vectors and HDR
433 oligos using Fugene6 according to manufacturer's guidelines (Promega #E2691). Following
434 transient puromycin-selection, single clones were picked and expanded as described previously⁴⁵.
435 Genotyping PCR was performed using primers (Forward: TACCCAGGAATGGCTTCTC;
436 Reverse: ACGTGTTCTGTTGTCCCA) to amplify targeted region followed by *AluI* restriction
437 digest. Successfully targeted clones were confirmed via Sanger sequence and monoallelic
438 sequencing was performed by TA-cloning (pGEM®-T Easy Vector System; Promega #A1360) of
439 the PCR amplicons. The control hiPSC line (p.Arg138Arg) was generated from hiPSC cells that
440 went through the CRISPR pipeline without being edited at the *SLC30A8* locus. The two p.Arg138*
441 clones (A3 and B1) and the unedited control line (p.Arg138Arg) passed quality control checks that
442 included repeat chromosome counting and pluripotency testing.

443 ***In vitro differentiation of hiPSCs towards Beta-like cells:*** Directed differentiation of hiPSCs
444 towards beta-like cells was performed using a previously published protocol^{14,46}. hiPSCs were
445 seeded on Growth Factor Reduced Matrigel-coated CellBind 12-well tissue culture plates (Corning
446 #356230 & #3336) at a cell density of 1.3×10^6 in mTesR1 (Stem Cell Technologies #05850) with
447 10 μ M Y-27632 dihydrochloride (Abcam #ab120129). The following morning, hiPSCs were fed
448 mTesR1 media >4 hours before starting the seven-stage differentiation protocol.

449 *Stage 1 (Definitive Endoderm)*: Cells were washed once with PBS before adding 0.5% bovine
450 serum albumin (BSA; Roche #10775835001) MCDB131 media [(ThermoFisher Scientific
451 #10372019) containing 1x Penicillin-Streptomycin (Sigma #P0781), 1.5 g/L sodium bicarbonate
452 (ThermoFisher Scientific #25080060), 1x GlutaMAX™ (ThermoFisher Scientific #35050038) and
453 10 mM Glucose (ThermoFisher Scientific #A2494001)] supplemented with 100 ng/mL Activin A
454 (PeproTech #120-14) and 3 μM CHIR 99021 (Axon Medchem #1386). On day 2 and 3, cells were
455 cultured with 0.5% BSA MCDB131 media supplemented with either 100 ng/mL Activin A and 0.3
456 μM CHIR 99021 (day 2) or with 100 ng/mL Activin A alone (day 3).

457 *Stage 2 (Primitive Gut Tube)*: Cells were cultured for 48 hours in 0.5% BSA MCDB131 media with
458 0.25 mM ascorbic acid (Sigma #A4544) and 50 ng/mL KGF (PeproTech #100-19).

459 *Stage 3 (Posterior Foregut)*: Cells were cultured for two days in 2% BSA MCDB131 media
460 supplemented with 1 g/L sodium bicarbonate, 0.25 mM ascorbic acid, 0.5x Insulin-Transferrin-
461 Selenium-Ethanolamine (ITS-X; ThermoFisher Scientific #51500056), 1 μM retinoic acid (RA;
462 Sigma-Aldrich #R2625), 0.25 μM Sant-1 (Sigma-Aldrich #S4572), 50 ng/ml KGF, 100 nM
463 LDN193189 (Stemgent #04-0074), and 100 nM α-Amyloid Precursor Protein Modulator (Merck
464 #565740).

465 *Stage 4 (Pancreatic Endoderm)*: Cells were cultured for three days in 2% BSA MCDB131 media
466 supplemented with 1 g/L sodium bicarbonate, 0.25 mM ascorbic acid, 0.5x ITS-X, 0.1 μM RA, 0.25
467 μM Sant-1, 2 ng/ml KGF, 200 nM LDN193189 and 100 nM α-Amyloid Precursor Protein
468 Modulator.

469 *Stage 5 (Endocrine Progenitors)*: Cells remained in planar culture for three days in 2% BSA
470 MCDB131 media supplemented with 20 mM final glucose, 0.5x ITS-X, 0.05 μM RA, 0.25 μM
471 Sant-1, 100 nM LDN193189, 10 μM ALK5 Inhibitor II (Enzo Life Sciences #ALX-270-445), 1 μM

472 3,3,5-Triiodo-L-thyronine sodium salt (T3; Sigma-Aldrich #T6397), 10 μ M zinc sulfate
473 heptahydrate (Sigma # Z0251), and 10 μ g/mL heparin sodium salt (Sigma #H3149).

474 Stage 6 (Endocrine Cells): Cells remained in planar culture for six days in 2% BSA MCDB131
475 media supplemented with 20 mM final glucose, 0.5x ITS-X, 100 nM LDN193189, 10 μ M ALK5
476 Inhibitor II, 1 μ M T3, 10 μ M zinc sulfate heptahydrate, and 100 nM γ -Secretase Inhibitor XX
477 (Merck Millipore #565789).

478 Stage 7 (Beta-like Cells): Cells remained in planar culture for another six days in 2% BSA
479 MCDB131 media supplemented with 20 mM final glucose, 0.5x ITS-X, 10 μ M ALK5 Inhibitor II,
480 1 μ M T3, 1 mM N-Cys (Sigma-Aldrich #A9165), 10 μ M Trolox (EMD Millipore #648471), 2 μ M
481 R248 (SelleckChem #S2841), and 10 μ M zinc sulfate heptahydrate.

482 ***Quantification of SLC30A8 gene expression in Beta-like Cells derived from CRISPR-edited***
483 ***hiPSCs:*** Expression of *SLC30A8* was measured at the end of stage 7 using quantitative PCR
484 (qPCR). Briefly, RNA was extracted using TRIzol Reagent (Life Technologies #15596026)
485 according to manufacturer's instructions. cDNA was amplified using the GoScript Reverse
486 Transcription Kit (Promega #A5000). qPCR was performed using 40 ng of cDNA, TaqMan® Gene
487 Expression Master Mix (Applied Biosystems #4369017) and primer/probes for *SLC30A8*
488 (Hs00545182_m1) or the housekeeping gene *TBP* (Hs00427620_m1). Gene expression was
489 determined using the $\Delta\Delta$ CT method by first normalizing to *TBP* and then to the control
490 p.Arg138Arg sample (n=6-7 wells from two differentiations).

491 ***Allele-specific SLC30A8 expression in Beta-like Cells derived from CRISPR-edited hiPSCs:***

492 Stage 7 cells were treated with 100 μ g/mL cycloheximide (Sigma #C4859) or DMSO (Sigma
493 #D2650) for four hours at 37°C⁴⁷ before harvesting for RNA and cDNA synthesis as above. Allele
494 specific expression was measured using the QX10 Droplet Digital PCR System and C1000 Touch
495 Thermal Cycler according to manufacturer's guidelines (Bio-Rad). Custom primers and probes for

496 the detection of p.Arg138* variant were designed using Primer3Plus (Applied Biosystems):
497 Forward primer AGTCTCTTCTCCCTGTGGTT; Reverse primer
498 ATGATCATCACAGTCGCCTG; FAM probe 5'-FAM-ATGGCACCGAGCTGA-MGB-3'; VIC
499 probe 5'-VIC-ATGGCACTGAGCTGAGA-MGB-3'. Results were analysed using Quanta Soft
500 software (Bio-Rad) and presented as a ratio of wildtype to HDR-edited allele expression (n>3 wells
501 from two differentiations).

502 **EndoC- β H1 culture**

503 The results obtained in EndoC- β H1 are from two distinct teams (Helsinki and Oxford) with
504 different batches of EndoC- β H1 cultures. Here, we report both methods and specify for each
505 experiment the origin of the culture (Helsinki or Oxford). EndoC- β H1 cells were cultured in
506 medium and grown on a matrix as described previously⁴⁸ and tested negative for mycoplasma.

507 ***SLC30A8 knockdown in EndoC- β H1 cells:*** In Oxford, EndoC- β H1 cells were transfected with 10
508 nM siRNA (either SMARTpool ON-TARGETplus SLC30A8 or scramble [Dharmacon #L-007529-
509 01]) and Lipofectamine RNAiMAX (Life Technologies #13778-075) according to manufacturer's
510 instructions for a total of 72 hours. In Helsinki, EndoC- β H1 cells were transfected using
511 Lipofectamin RNAiMAX (life technologies). 20nM siRNA ON-TARGET^{plus} siRNA SMARTpool
512 for human *SLC30A8* gene (Dharmacon; L-007529-01) and ON-TARGET^{plus} Non-targeting pool
513 (siNT or Scramble) (Dharmacon; D-001810-10-05) were used following the protocol as described
514 previously⁴⁹. Cells were harvested 96 h post-transfection for further studies.

515 ***Insulin secretion measurements in EndoC- β H1 cells:*** In Oxford, cells were subjected to static
516 insulin secretion assays 72hrs after siRNA transfection as described previously⁵⁰, apart from the
517 following modifications: cells were stimulated for 1 hr with 1 mM glucose, 20 mM glucose, 1 mM
518 glucose + 200 μ M tolbutamide, or 20 mM glucose + 500 μ M diazoxide. Insulin levels were
519 measured in both supernatants and cells using the Insulin (human) AlphaLISA Detection Kit and

520 EnSpire Alpha Plate Reader (Perkin Elmer #AL204C and #2390-0000, respectively). Cell count per
521 well was measured via CyQUANT Direct Cell Proliferation Assay (Thermo Fisher# C35011). Data
522 are presented as insulin secretion normalized to percentage of insulin content from Control
523 condition. RNA extraction, cDNA synthesis, and qRT-PCR was performed as above (*SLC30A8*
524 gene expression in CRISPR-edited hiPSCs derived beta like cell section) to determine *SLC30A8*
525 knockdown and expression of the K_{ATP} channel genes (*ABCC8* Hs01093752_m1 and *KCNJ11*
526 Hs00265026_s1; ThermoFisher Scientific). In Helsinki, EndoC- β H1 cells were transfected with
527 20nM siRNA and Scramble control. Following 96h of siRNA transfection, cells were incubated
528 overnight in 1 mM glucose containing EndoC- β H1 culture medium. One hour prior to glucose
529 stimulation assay, the media was replaced by β KREBS (Univercell Biosolution S.A.S., France)
530 without glucose. Cells were stimulated with 16.7 mM glucose and 50 mM KCl (Sigma-Aldrich) in
531 β KREBS for 30 min at 37°C in a CO₂ incubator. The cells were then washed and lysed with TETG
532 (Tris pH8, Trito X-100, Glycerol, NaCl and EGTA) solution (Univercell Biosolution S.A.S.,
533 France) for the measurement of total insulin content. Secreted and intracellular insulin were
534 measured using a commercial human insulin Elisa kit (Mercoxia AB, Uppsala, Sweden) as per
535 manufacturer's instructions (Helsinki).

536 ***Electrophysiological measurements in EndoC- β H1 cells (Oxford):*** *SLC30A8* was knocked down
537 in EndoC- β H1 as above. K_{ATP} channel conductance was measured in a perforated patch whole cell
538 configuration, and patch-clamped using an EPC 10 amplifier and HEKA pulse software. KREBS
539 extracellular solution was perfused in at 32°C and contained: 138 mM NaCl, 3.6 mM KCl, 0.5 mM
540 MgSO₄, 10 mM HEPES, 0.5 mM NaH₂PO₄, 5 mM NaHCO₃, 1.5 mM CaCl₂, 1 mM glucose and 100
541 μ M Diazoxide (Sigma-Aldrich #D9035). The perforation of the membrane was achieved using an
542 intra-pipette solution containing: 0.24 mg/mL amphotericin B, 128 mM K-gluconate (Sigma
543 #Y0000005 and G4500 respectively), 10 mM KCl, 10 mM NaCl, 1 mM MgCl₂, 10 mM HEPES,
544 pH 7.35 (KOH). Conductance data are normalised to cell size and presented as pS.pF⁻¹. Expression

545 of *ABCC8*, *KCNJ11*, *B2M*, and *TBP* were measured via qPCR as above (*SLC30A8* gene expression
546 in CRISPR-edited hiPSCs derived beta like cell section).

547 ***Insulin and Proinsulin secretion and content (Helsinki):*** For the measurement of secreted insulin
548 or proinsulin in the supernatant, 96h post-transfected cells were washed twice with 1X PBS and
549 incubated with fresh EndoC- β H1 culture medium for next 24h. Secreted and intracellular insulin
550 and proinsulin were measured using a commercial human insulin Elisa and human proinsulin Elisa
551 kit from Merckodia (Merckodia AB, Uppsala, Sweden). Total cellular protein content was also
552 determined with the BCA protein assay kit (Thermo Scientific, Pierce). Proinsulin to insulin ratio
553 was calculated by dividing the respective values measured from the supernatant and the cells
554 (pmol/L).

555 ***Immunoblotting (Helsinki):*** Total cellular protein was prepared with Laemmli buffer and resolved
556 using Any kD Mini-Protean-TGX gel (Bio-Rad). Immunoblot analysis was performed by overnight
557 incubation of with primary antibodies against ZNT8 (Abcam; #ab136990; 1:500), PC1/3 (Cell
558 Signaling; #11914; 1:1000), CPE (BD Bioscience; #610758; 1:1000), Phospho-AKT-Ser473 (Cell
559 Signaling; #4060; 1:1000), AKT (Santa-Cruz; #SC-8312; 1:500). The membranes were further
560 incubated with species-specific HRP-linked secondary antibodies (1:5000) and visualization was
561 performed following ECL exposure with ChemiDoc XRS+ system and Image Lab Software (Bio-
562 Rad). A loading control of either alpha-Tubulin (Sigma; T5168; 1:5000) or beta-actin (Sigma;
563 A5441; 1:5000) was performed on the same blot for all western blot data. Densitometric analysis of
564 bands from image were calculated using Image J (Media Cybernetics) software and intensities
565 compared as ZNT8, PC1/3, phosphor-AKT-Ser473 to tubulin; CPE to beta-actin.

566 ***Cell viability assay, MTT (Helsinki):*** EndoC- β H1 cells were transfected with either siScramble or
567 siSLC30A8 for 96h. The viability of cells after 24 h of tunicamycin (10 μ g/ml) treatment was
568 determined using Vybrant MTT Cell proliferation kit (ThermoFisher Scientific; #M6494), the

569 standard MTT [3-(4,5-dimethylthiazol-2-yl)-2,5-diphenyltetrazolium bromide] assay. All the
570 treatments were performed on cells with equal seeding density (5×10^4 cells/well) in 96 wells plate.
571 The purple formazan crystals generated after 2 h incubation with MTT buffer were dissolved in
572 DMSO, and the absorbance was recorded on a microplate reader at a wavelength of 540nm.

573 **RNA (mRNAs) sequencing of EndoC- β H1 cells:** For RNA sequencing post 96h siScramble
574 (n=3) or siSLC30A8 (n=3) transfected EndoC- β H1 cells were used and the total RNA was
575 extracted with Macherey-Nagel RNA isolation kit as per manufacturer's instruction. RNA
576 sequencing was performed using Illumina TruSeq-mRNA library on NextSeq 500 system (Illumina)
577 with an average of >15 million paired-end reads (2×75 base pairs). RNA sequencing reads were
578 aligned to hg38 using STAR (Spliced Transcripts Alignment to Reference)⁵¹, genome annotations
579 were obtained from the GENCODE (Encyclopedia of Genes and Gene Variants) v22⁵² program, and
580 reads counting were done using featureCounts⁵³. Further downstream analysis was perform using
581 edgeR⁵⁴ software package, low expressed (<1 average count per million) genes were removed, read
582 counts were normalized using TMM⁵⁵ (trimmed mean of M-values), differential expression analysis
583 was performed using method similar to Fisher's Exact Test and corrected for multiple testing using
584 FDR (1%).

585 **Data Analyses:** Data are reported as mean (SEM). Statistical analyses were performed using Prism
586 6.0 (GraphPad Software). All parameters were analyzed using Mann-Whitney test or Unpaired
587 Student's t-test as indicated.

588 **Mouse Model**

589 **Animals:** All procedures were conducted in compliance with protocols approved by the Regeneron
590 Pharmaceuticals Institutional Animal Care and Use Committee. The *Slc30a8*^{Tgp.Arg138*} mouse line is
591 made in pure C57Bl/6 background by changing nucleotide 409 from T into C in exon 3, which
592 changes the arginine into a stop codon¹¹. The mutated allele has a self-deleting neomycin selection

593 cassette flanked by loxP sites inserted at intron 3, deleting 29 bp of endogenous intron 3 sequence.
594 Mice were housed (up to five mice per cage) in a controlled environment (12-h light/dark cycle,
595 22C, 60–70% humidity) and fed *ad libitum* with either chow (Purina Laboratory 23 Rodent Diet
596 5001, LabDiet) or high-fat diet (Research Diets, D12492; 60% fat by calories) starting at age of 20
597 weeks. All data shown are compared to their respective WT littermates.

598 **Glucose Tolerance Test:** Mice were fasted overnight (16 hr) followed by oral gavage of glucose
599 (Sigma) at 2 g/kg body weight. Blood samples were obtained from the tail vein at the indicated
600 times and glucose levels were measured using the AlphaTrak2 glucometer (Abbott). Submandibular
601 bleeds for insulin were done at 0, 15, and 30 min post-injection.

602 **Hormone measurements:** Submandibular bleeds of either overnight fasted or fed animals were
603 done in the morning. Plasma insulin or proinsulin was analyzed with the mouse insulin/proinsulin
604 EIA (Mercodia AB, Uppsala, Sweden), and C-peptide with the mouse C-peptide EIA (ALPCO). All
605 EIAs were performed according to the manufacturer's instructions.

606 **Data Analyses for mouse studies:** Data are reported as mean (SEM). Statistical analyses were
607 performed using Prism 6.0 (GraphPad Software). All parameters were analyzed by two-way
608 ANOVA or Unpaired Student's t-test as indicated.

609 **Expression of p.Arg138* mutation in INS1E**

610 INS-1E cells⁵⁶ were used for transient transfection of pcDNA3.1(+)-p.Arg138* construct fused to
611 fluorescent m-Cherry at C-terminus using transfection reagent Viromer according to the
612 manufacturer's instructions. After transfections cells were collected at 24, 48, 72 and 96 hours and
613 analysed by western blot analysis using mCherry (600-401-P16, Rockland) antibody. Untransfected
614 cells were used as control and tubulin as a loading control. Two days after transient transfections
615 with either p.Arg138*-mCherry (INS1E), p.Arg138*-HA or p.Arg138*-Myc-His construct
616 (INS1E), cells were washed with PBS twice and fixed using 4% paraformaldehyde for 15 min at

617 room temperature. Cells were permeabilized with 0.2 % Triton X-100 in phosphate-buffered saline
618 (PBS) for 10 mins and to prevent unspecific binding were further blocked for 1 h with 5% FBS in
619 PBS. INS1E cells transfected with either p.Arg138*-HA or p.Arg138*-Myc-His construct were
620 incubated with the primary antibody (HA antibody: MMS-101P, Biolegend; His antibody: D291-
621 A48, MBL; insulin antibody: A0564, DAKO), overnight at 4°C. Secondary antibodies were
622 conjugated to Alexa Fluor 488 (Molecular Probes). Cells transfected with mCherry construct were
623 imaged after 48 and 96 hours (INS1E) in order to visualize subcellular localization at different time
624 points.

625 **Measurements of cytosolic zinc in INS-1(832/13) cells**

626 **Cell culture:** INS-1 (823/13) cells were grown in RPMI 1640 medium (Sigma-Aldrich, UK)
627 supplemented with 10% (v/v) foetal bovine serum (FBS), 2 Mm L-glutamine, 0.05 mM 2-
628 mercaptoethanol, 10 mM HEPES (Sigma-Aldrich), 1 mM sodium pyruvate (GIBCO, France), 2
629 mM L-glutamine and antibiotics (100 µg/ml Streptomycin and 100 U/ml penicillin). Cells were
630 maintained in 95% oxygen, 5% carbon dioxide at 37°C.

631 **Co-transfection:** Cells were seeded on sterile coverslips at 60% confluence and co-transfected
632 using lipofectamine 2000 (Invitrogen, USA) according to the manufacturer's instructions, with
633 either the empty construct (EV) or the rare-truncated variant (c-Myc tag, R138X) construct and the
634 Förster Resonance Energy transfer sensors (FRET), eCALWY-4 vector (free cytosolic zinc
635 measurements).

636 **Protein extraction and Western (immuno-) blotting analysis:** For protein extraction, RIPA buffer
637 (1% Triton X-100, 1% sodium deoxycholate, 0.1% SDS, 0.15 mM NaCl, 0.01 M sodium Phosphate
638 pH7.2) was used for lysis. Protein extracts were resolved in SDS-page (12% vol/vol acrylamide)
639 and transferred to a polyvinylidene fluoride (PVDF) membrane, followed by blocking for 1 hour,
640 immunoblotting with either c-Myc anti-mouse SLC30A8 (1:400) and the secondary anti-mouse

641 antibody (1:10000, Abcam), and then the mouse monoclonal anti-tubulin (1:10000) and secondary
642 anti-mouse for tubulin (1:5000). Chemiluminescence detection reagent (GE Healthcare) was used
643 before exposing to hyperfilms.

644 **Immunocytochemistry:** Cells were fixed in 4% (v/v) Phosphate-buffered saline/Paraformaldehyde
645 (PFA). Cells were permeabilized in 0.5% (w/v) PBS/TritonX-100 and further saturated with
646 PBS/BSA 0.1%. Cells were then incubated for 1 hour with the primary antibody, anti-c-Myc mouse
647 antibody (1:200) followed by the secondary Alexa Fluor® 568 nm anti-mouse IgG (H+L, 1:1000
648 Life Technologies, USA). Coverslips were mounted with mounting medium containing DAPI
649 (Vectashield, USA) on microscope slides (ThermoScientific). Imaging was performed on a Nikon
650 Eclipse Ti microscope equipped with a 63x/1.4NA objective, spinning disk (CAIRN, UK) using a
651 405, 488 and 561 nm laser lines, and images were acquired with an ORCA-Flash 4.0 camera
652 (Hamamatsu) Metamorph software (Molecular Device) was used for data capture.

653 **Cytosolic free Zn²⁺ measurements:** Acquisitions were performed 24 hours after transfection using
654 an Olympus IX-70 wide-field microscope with a 40x/1.35NA oil immersion objective and a zyla
655 sCMOS camera (Andor Technology, Belfast, UK) controlled by Micromanager software. Excitation
656 was provided at 433 nm using a monochromator (Polychrome IV, Till Photonics, Munich,
657 Germany). Emitted light was split and filtered with a Dual-View beam splitter (Photometrics,
658 Tucson, Az, USA) equipped with a 505dxcn dichroic mirror and two emission filters (Chroma
659 Technology, Bellows Falls, VT, USA - D470/24 for cerulean and D535/30 for citrine). Cells were
660 perfused for 4 minutes with KREBS buffer (140 mM NaCl, 3.6 mM KCl, 0.5 mM NaH₂PO₄, 0.2
661 mM MgSO₄, 1.5 mM CaCl₂, 10 mM HEPES, 25 mM NaHCO₃) without additives, next the buffer
662 was changed to KREBS buffer containing 50 μM N,N,N',N'-tetrakis(2-
663 pyridylmethyl)ethylenediamine (TPEN, Sigma) for 5 minutes, followed by perfusion with KREBS
664 buffer containing 100 μM ZnCl₂ and 5 μM of the Zn²⁺-specific ionophore 2-mercaptopyridine N-
665 oxide (Pyrithione, Sigma). Image analysis was performed using ImageJ software. Steady-state

666 fluorescence intensity ratio of acceptor over donor was measured, followed by the determination of
667 the minimum and maximum ratios to calculate the free Zn^{2+} concentration using the following
668 formula: $[Zn^{2+}] = Kd \cdot (R - R_{min}) / (R_{max} - R)$, in which R_{min} is the ratio in the Zn^{2+} depleted
669 state, after addition of $50 \mu M$ TPEN, and R_{max} was obtained upon Zn^{2+} saturation with $100 \mu M$
670 $ZnCl_2$ in the presence of $5 \mu M$ pyritnone.

671 **Human Pancreatic islets**

672 Experiments on primary human pancreatic islets were independently performed in two places 1)
673 Oxford and 2) Lund university diabetes center (LUDC)

674 ***Human pancreatic islets from Oxford:*** Human pancreatic islets were isolated from deceased
675 donors under ethical approval obtained from the human research ethics committees in Oxford
676 (REC: 09/H0605/2, NRES committee South Central-Oxford B). All donors gave informed research
677 consent as part of the national organ donation program. Islets were obtained from the Diabetes
678 Research & Wellness Foundation Human Islet Isolation Facility, OCDEM, University of Oxford.
679 All methods and protocols using human pancreatic islets were performed in accordance with the
680 relevant guidelines and regulations in the UK (Human Tissue Authority, HTA). Expression data for
681 *SLC30A8* estimated by RNA sequencing as described previously⁵⁷. For *in vitro* insulin secretion,
682 islets were pre-incubated in Krebs-Ringer buffer (KRB) containing 2 mg/mL BSA and 1 mM
683 glucose for 1 hour at 37°C, followed by 1-hour stimulation in KRB supplemented with 6mM
684 glucose. Insulin content of the supernatant was determined by radioimmunoassay (Millipore UK
685 Ltd, Livingstone, UK) as described previously⁵⁸.

686 ***Human pancreatic islets from LUDC:*** Human pancreatic islets were obtained from the Human
687 Tissue Laboratory (Lund University, www.exodiab.se/home) in collaboration with The Nordic
688 Network for Clinical Islet Transplantation Program (www.nordicislets.org)^{59,60}. All the islet donors
689 provided their consent for donation of organs for medical research and the procedures were

690 approved by the ethics committee at Lund University (Malmö, Sweden, permit number 2011263).
691 Islet preparation for cadaver donors, their purity check and counting procedure have been described
692 previously⁶¹. Static *in vitro* insulin secretion assay from 91 islets (non-diabetic individuals) was
693 performed as described previously^{61,62}. Briefly, six batches of 12 islets per donor were incubated for
694 1 hour at 37°C in Krebs Ringer bicarbonate (KRB) buffer in presence of 1 mM or 16.7 mM
695 glucose, as well as 1 mM or 16.7 mM glucose together with 70 mM KCl. Insulin concentrations in
696 the extracts was measured using a radioimmunoassay kit (Euro-Diagnostica, Malmö, Sweden). The
697 Association of p.Trp325Arg genotype with expression of *SLC30A8* and other genes involved in
698 insulin production and processing²² was performed using RNA sequencing from islets of 140 non-
699 diabetic individuals as described previously^{59,60}. Briefly, RNA sequencing of islets was done using
700 a HiSeq 2000 system (Illumina) for an average depth of 32.4 million paired-end reads (2 × 100 base
701 pairs)^{59,60}. RNA sequencing reads were aligned to hg19 using STAR (Spliced Transcripts
702 Alignment to Reference)⁵¹. Genome annotations were obtained from the GENCODE (Encyclopedia
703 of Genes and Gene Variants) v20⁵² program and read counting was done using featureCounts⁵³.
704 Read counts were normalized to total reads (counts per million) and additionally across-samples
705 normalization was done using TMM method⁵⁵. Association analysis (so called eQTL) was
706 performed on inverse normalized expression values using linear regression adjusted for age, sex and
707 islets purity.

708 **Statistics**

709 Detail information regarding statistical tests used for each sub-study has been provided in their
710 respective method section or with figure legends.

711 **Data availability**

712 The data that support the findings of this study are available from the corresponding author on
713 reasonable request. Individual level data for the human study can only be obtained via the Biobank
714 of The Institute of Health and Welfare in Finland.

715
716
717

718 References

- 719 1. Chabosseau, P., & Rutter, G.A. Zinc and diabetes. *Arch Biochem Biophys* **611**, 79-85 (2016).
- 720 2. Chimienti, F., Devergnas, S., Favier, A., & Seve, M. Identification and cloning of a beta-cell-specific zinc
721 transporter, ZnT-8, localized into insulin secretory granules. *Diabetes* **53**, 2330-7 (2004).
- 722 3. Flannick, J. et al. Loss-of-function mutations in SLC30A8 protect against type 2 diabetes. *Nat Genet* **46**, 357-63
723 (2014).
- 724 4. Flannick, J. et al. Genetic discovery and translational decision support from exome sequencing of 20,791 type 2
725 diabetes cases and 24,440 controls from five ancestries *bioRxiv* (2018).
- 726 5. Parsons, D.S., Hogstrand, C., & Maret, W. The C-terminal cytosolic domain of the human zinc transporter ZnT8
727 and its diabetes risk variant. *FEBS J.* **285**, 1237-1250 (2018).
- 728 6. Sladek, R. et al. A genome-wide association study identifies novel risk loci for type 2 diabetes. *Nature* **445**, 881-5
729 (2007).
- 730 7. Lemaire, K. et al. Insulin crystallization depends on zinc transporter ZnT8 expression, but is not required for
731 normal glucose homeostasis in mice. *Proc Natl Acad Sci U S A* **106**, 14872-7 (2009).
- 732 8. Pound, L.D. et al. Deletion of the mouse Slc30a8 gene encoding zinc transporter-8 results in impaired insulin
733 secretion. *Biochem J* **421**, 371-6 (2009).
- 734 9. Wijesekara, N. et al. Beta cell-specific Znt8 deletion in mice causes marked defects in insulin processing,
735 crystallisation and secretion. *Diabetologia* **53**, 1656-68 (2010).
- 736 10. Mitchell, R.K. et al. Molecular Genetic Regulation of Slc30a8/ZnT8 Reveals a Positive Association with Glucose
737 Tolerance. *Mol Endocrinol.* **30**, 77-91 (2016).
- 738 11. Kleiner, S. et al. Mice harboring the human SLC30A8 R138X loss-of-function mutation have increased insulin
739 secretory capacity. *Proc Natl Acad Sci* **115(32)**, E7642-E7649 (2018).
- 740 12. Groop, L. et al. Metabolic consequences of a family history of NIDDM (the Botnia study): evidence for sex-
741 specific parental effects. *Diabetes* **45**, 1585-93 (1996).
- 742 13. Tamaki, M. et al. The diabetes-susceptible gene SLC30A8/ZnT8 regulates hepatic insulin clearance. *J Clin Invest*
743 **123**, 4513-24 (2013).
- 744 14. Rezanian, A. et al. Reversal of diabetes with insulin-producing cells derived in vitro from human pluripotent stem
745 cells. *Nat Biotechnol* **32**, 1121-33 (2014).
- 746 15. Miyaoka, Y., Chan, A.H., & Conklin, B.R. Using Digital Polymerase Chain Reaction to Detect Single-Nucleotide
747 Substitutions Induced by Genome Editing. *Cold Spring Harb Protoc* (2016).
- 748 16. Scharfmann, R. et al. Development of a conditionally immortalized human pancreatic β cell line. *J Clin Invest*
749 **124**, 2087-98 (2014).
- 750 17. Hastoy, B. et al. Electrophysiological properties of human β -cell lines EndoC- β H1 and - β H2 conform with
751 human β -cells. *BioRxiv* (2017).
- 752 18. Braun, M. et al. Voltage-gated ion channels in human pancreatic beta-cells: electrophysiological characterization
753 and role in insulin secretion. *Diabetes* **57**, 1618-28 (2008).
- 754 19. Srinivasan, S., Bernal-Mizrachi, E., Ohsugi, M., & Permutt, M.A. Glucose promotes pancreatic islet beta-cell
755 survival through a PI 3-kinase/Akt-signaling pathway. *Am J Physiol Endocrinol Metab* **283**, E784-93 (2002).
- 756 20. Nicolson, T.J. et al. Insulin storage and glucose homeostasis in mice null for the granule zinc transporter ZnT8
757 and studies of the type 2 diabetes-associated variants. *Diabetes* **58**, 2070-83 (2009).
- 758 21. Vinkenborg, J.L. et al. Genetically encoded FRET sensors to monitor intracellular Zn²⁺ homeostasis. *Nat*
759 *Methods* **6**, 737-40 (2009).
- 760 22. Zhou, Y. et al. TCF7L2 is a master regulator of insulin production and processing. *Hum Mol Genet* **23**, 6419-31
761 (2014).
- 762 23. Kirchhoff, K. et al. Polymorphisms in the TCF7L2, CDKAL1 and SLC30A8 genes are associated with impaired
763 proinsulin conversion. *Diabetologia* **51**, 597-601 (2008).

- 764 24. Jainandunsing, S. et al. A stable isotope method for in vivo assessment of human insulin synthesis and secretion.
765 *Acta Diabetol* **53**, 935-944 (2016).
- 766 25. Ivanova, A. et al. Age-dependent labeling and imaging of insulin secretory granules. *Diabetes* **62**, 3687-96
767 (2013).
- 768 26. Gerber, P.A. et al. Hypoxia lowers SLC30A8/ZnT8 expression and free cytosolic Zn²⁺ in pancreatic beta cells.
769 *Diabetologia* **57**, 1635-44 (2014).
- 770 27. Wong, W.P. et al. Exploring the Association Between Demographics, SLC30A8 Genotype, and Human Islet
771 Content of Zinc, Cadmium, Copper, Iron, Manganese and Nickel. *Sci Rep* **7** (1), 473 (2017).
- 772 28. Vergnano, A.M. et al. Zinc dynamics and action at excitatory synapses. *Neuron* **82**, 1101-14 (2014).
- 773 29. Prost, A.L., Bloc, A., Hussy, N., Derand, R., & Vivaudou, M. Zinc is both an intracellular and extracellular
774 regulator of KATP channel function. *J Physiol* **559**, 157-67 (2004).
- 775 30. Ferrer, R., Soria, B., Dawson, C.M., Atwater, I., & Rojas, E. Effects of Zn²⁺ on glucose-induced electrical
776 activity and insulin release from mouse pancreatic islets. *Am J Physiol* **246**, C520-7 (1984).
- 777 31. Isomaa, B. et al., A family history of diabetes is associated with reduced physical fitness in the Prevalence,
778 Prediction and Prevention of Diabetes (PPP)-Botnia study. *Diabetologia* **53**, 1709-13 (2010).
- 779 32. Ahlqvist, E. et al. Novel subgroups of adult-onset diabetes and their association with outcomes: a data-driven
780 cluster analysis of six variables. *Lancet Diabetes Endocrinol* **6**, 361-369 (2018).
- 781 33. Lindgren, O. et al. Incretin hormone and insulin responses to oral versus intravenous lipid administration in
782 humans. *J Clin Endocrinol Metab* **96**, 2519-24 (2011).
- 783 34. Sluiter, W.J., Erkelens, D.W., Reitsma, W.D. & Doorenbos, H. Glucose tolerance and insulin release, a
784 mathematical approach I. Assay of the beta-cell response after oral glucose loading. *Diabetes* **25**, 241-4 (1976).
- 785 35. Mohandas, C. et al. Ethnic differences in insulin secretory function between black African and white European
786 men with early type 2 diabetes. *Diabetes Obes Metab* **20**, 1678-1687 (2018).
- 787 36. Navalesi, R., Pilo, A. & Ferrannini, E. Kinetic analysis of plasma insulin disappearance in nonketotic diabetic
788 patients and in normal subjects. A tracer study with 125I-insulin. *J Clin Invest* **61**, 197-208 (1978).
- 789 37. Delaneau, O., Zagury, J.F. & Marchini, J. Improved whole-chromosome phasing for disease and population
790 genetic studies. *Nat Methods* **10** (1), 5-6 (2013).
- 791 38. Flannick, J. et al. Sequence data and association statistics from 12,940 type 2 diabetes cases and controls. *Sci*
792 *Data* **4**, 170179 (2017).
- 793 39. Howie, B., Fuchsberger, C., Stephens, M., Marchini, J. & Abecasis G.R. Fast and accurate genotype imputation
794 in genome-wide association studies through pre-phasing. *Nat Genet* **44**, 955-9 (2012)
- 795 40. Abecasis, G.R., Cardon, L.R., & Cookson, W.O. A general test of association for quantitative traits in nuclear
796 families. *Am J Hum Genet* **66**, 279-92 (2000).
- 797 41. Yang, J., Lee, S.H., Goddard, M.E. & Visscher, P.M. GCTA: a tool for genome-wide complex trait analysis. *Am*
798 *J Hum Genet* **88**, 76-82 (2011).
- 799 42. Bonetti, S. et al. Variants of GCKR affect both β -cell and kidney function in patients with newly diagnosed type
800 2 diabetes: the Verona newly diagnosed type 2 diabetes study 2. *Diabetes Care* **34**, 1205-10 (2011).
- 801 43. van de Bunt, M. et al. Insights into islet development and biology through characterization of a human iPSC-
802 derived endocrine pancreas model. *Islets* **8**, 83-95 (2016).
- 803 44. Cong, L. et al. Multiplex genome engineering using CRISPR/Cas systems. *Science* **339**, 819-23 (2013).
- 804 45. Krentz, N.A.J. et al. Phosphorylation of NEUROG3 Links Endocrine Differentiation to the Cell Cycle in
805 Pancreatic Progenitors. *Dev Cell* **41**, 129-142.e6 (2017).
- 806 46. Perez-Alcantara, M. et al. Patterns of differential gene expression in a cellular model of human islet development,
807 and relationship to type 2 diabetes predisposition. *Diabetologia* **61**, 1614-1622 (2018).
- 808 47. Harries, L.W., Hattersley, A.T. & Ellard S. Messenger RNA transcripts of the hepatocyte nuclear factor-1alpha
809 gene containing premature termination codons are subject to nonsense-mediated decay. *Diabetes* **53**, 500-4
810 (2004).
- 811 48. Ravassard, P. et al. A genetically engineered human pancreatic β cell line exhibiting glucose-inducible insulin
812 secretion. *J Clin Invest* **121**, 3589-97 (2011).
- 813 49. Chandra, V. et al. RFX6 regulates insulin secretion by modulating Ca²⁺ homeostasis in human β cells. *Cell Rep*
814 **9**, 2206-18 (2014).
- 815 50. Thomsen, S.K. et al. Systematic Functional Characterization of Candidate Causal Genes for Type 2 Diabetes Risk
816 Variants. *Diabetes* **65**, 3805-3811 (2016).
- 817 51. Dobin, A. et al. STAR: ultrafast universal RNA-seq aligner. *Bioinformatics* **29**, 15-21 (2013).
- 818 52. Harrow, J. et al. GENCODE: the reference human genome annotation for The ENCODE Project. *Genome Res.*
819 **22**, 1760-74 (2012).
- 820 53. Liao, Y., Smyth, G.K. & Shi, W. featureCounts: an efficient general purpose program for assigning sequence
821 reads to genomic features. *Bioinformatics* **30**, 923-30 (2014).
- 822 54. Robinson, M.D., McCarthy, D.J. & Smyth G.K. "edgeR: a Bioconductor package for differential expression
823 analysis of digital gene expression data." *Bioinformatics*, **26**, 139-140 (2010).

- 824 55. Robinson, M.D. & Oshlack, A. A scaling normalization method for differential expression analysis of RNA-seq
825 data. *Genome Biol.* **11**, R25 (2010).
- 826 56. Asfari, M. et al. Establishment of 2-mercaptoethanol-dependent differentiated insulin-secreting cell lines.
827 *Endocrinology* **130**, 167-78 (1992).
- 828 57. van de Bunt, M. et al. Transcript Expression Data from Human Islets Links Regulatory Signals from Genome-
829 Wide Association Studies for Type 2 Diabetes and Glycemic Traits to Their Downstream Effectors. *PLoS Genet.*
830 **11**(12), e1005694 (2015).
- 831 58. Ramracheya, R. et al. Membrane potential-dependent inactivation of voltage-gated ion channels in alpha-cells
832 inhibits glucagon secretion from human islets. *Diabetes* **59**, 2198-208 (2010).
- 833 59. Ottosson-Laakso, E. et al. Glucose-Induced Changes in Gene Expression in Human Pancreatic Islets: Causes or
834 Consequences of Chronic Hyperglycemia. *Diabetes* **66**, 3013-3028 (2017).
- 835 60. Fadista, J. et al. Global genomic and transcriptomic analysis of human pancreatic islets reveals novel genes
836 influencing glucose metabolism. *Proc Natl Acad Sci U S A* **111**, 13924-9 (2014).
- 837 61. Rosengren, A.H. et al. Overexpression of alpha2A-adrenergic receptors contributes to type 2 diabetes. *Science.*
838 **327**, 217-20 (2010).
- 839 62. Taneera, J. et al. Identification of novel genes for glucose metabolism based upon expression pattern in human
840 islets and effect on insulin secretion and glycemia. *Hum Mol Genet* **24**, 1945-55 (2015).

841

842 **URLs**

843

844 GCTA, <http://cns.genomics.com/software/gcta>; SHAPEIT,
845 http://mathgen.stats.ox.ac.uk/genetics_software/shapeit/shapeit.html, IMPUTE2,
846 http://mathgen.stats.ox.ac.uk/impute/impute_v2.html;

847

848 **Acknowledgements**

849

850

851

852

853

854

855

856

857

858

859

860

861

862

863

864

865

866

867

868

869

870

871

872

873

874

875

876

877

We thank the Botnia Study Group for recruiting and studying the participants, Jens Juul Holst for measuring GLP-1 concentrations, and Linda Boselli, PhD, for carrying out mathematical modelling of the OGTT studies. We thank Erqian Na for her help with the mouse immunohistochemistry and histology, and Catherine Green and the Chromosome Dynamics & Genome Engineering Cores at the Wellcome Centre for Human Genetics for support with karyotyping and genome editing (funded by the Wellcome Trust grant 203141). The Botnia and The PPP-Botnia studies (L.G., T.T.) have been financially supported by grants from Folkhälsan Research Foundation, the Sigrid Juselius Foundation, The Academy of Finland (grants no. 263401, 267882, 312063 to LG, 312072 to TT), Nordic Center of Excellence in Disease Genetics, EU (EXGENESIS, EUFP7-MOSAIC FP7-600914), Ollqvist Foundation, Swedish Cultural Foundation in Finland, Finnish Diabetes Research Foundation, Foundation for Life and Health in Finland, Signe and Ane Gyllenberg Foundation, Finnish Medical Society, Paavo Nurmi Foundation, Helsinki University Central Hospital Research Foundation, Perklén Foundation, Närpes Health Care Foundation and Ahokas Foundation, as well as by the Ministry of Education in Finland, Municipal Health Care Center and Hospital in Jakobstad and Health Care Centers in Vasa, Närpes and Korsholm. The work described in this paper has been supported with funding from collaborative agreements with Pfizer Inc., as well as with Regeneron Genetics Center LLC. J.L. was supported by Vinnova - Sweden's Innovation Agency (2015-01549), Swedish Diabetes Foundation, Albert Pålsson Foundation, Hjelt Foundations, Crafoord Foundation, Royal Physiographic Society in Lund, Swedish Foundation for Strategic Research (IRC15-0067), Swedish Research council (2009-1039, Strategic research area Exodiab); E.A. by Crafoord Foundation, Pålsson Foundation, Swedish Research Council (Dnr: 2017-02688).; O.H. by Lund University Diabetes Center, ALF, Crafoord foundation, Novo Nordisk foundation, Magnus Bergvall foundation, Pålsson foundation, Diabetes Wellness and Swedish Diabetes Research Foundation; R.C.B. by Italian Ministry of University and Research (PRIN 2015373Z39_004) and University of Parma Research Funds; G.R. by a Wellcome Trust Senior Investigator Award (WT098424AIA), MRC Programme grants (MR/R022259/1, MR/J0003042/1, MR/L020149/1) and Experimental Challenge Grant (DIVA, MR/L02036X/1), MRC (MR/N00275X/1), Diabetes UK (BDA/11/0004210, BDA/15/0005275, BDA 16/0005485) and Imperial Confidence in Concept (ICiC) grants, and a Royal Society Wolfson Research Merit Award. ALG is a Wellcome Trust

878 Senior Fellow in Basic Biomedical Science. M.I.M. and P.R. are Wellcome Senior
879 Investigators. This work was funded in Oxford by the Wellcome Trust (095101 [ALG], 200837
880 [A.L.G.], 098381 [M.I.M.], 106130 [A.L.G., M.I.M.], 203141 (A.L.G., B.D., M.I.M.), 203141
881 [M.I.M.], 090531 [P.R.]), Medical Research Council (MR/L020149/1) [M.I.M., A.L.G., P.R.],
882 European Union Horizon 2020 Programme (T2D Systems) [A.L.G.], and NIH (U01-DK105535;
883 U01-DK085545) [M.I.M., A.L.G.]. The research was funded by the National Institute for Health
884 Research (NIHR) Oxford Biomedical Research Centre (BRC) [A.L.G., M.I.M., P.R.]. The views
885 expressed are those of the author(s) and not necessarily those of the NHS, the NIHR or the
886 Department of Health.

887

888 **Author Contributions**

889 M.L., L.S., T.T. and L.G. conducted the human study; E.A., O.H., A.B. and J.F. analyzed the
890 genotype data ; M.L., O.P.D., M.T., E.B., R.C.B, T.T. and L.G. analyzed the human data; B.H.,
891 N.L.B., S.K.T., M.vD.B., V.C., O.P.D., T.O. and A.L.G. characterized the Human beta-cell model;
892 N.L.B., N.A.J.K., F.A., B.C., D.M., P.K., B.D., M.I.M. and A.L.G. characterized the human IPS
893 cell derived model; U.K., R.P., O.P.D., B.H., A.J.P., I.S., R.R., I.A., P.R., M.I.M. and A.L.G.
894 characterized the human islets; S.K., D.G. and J.G. characterized the *Slc30a8* p.Arg138* mice; D.J.,
895 J.L., P.C., A.T., R.C., A-M.R., J.B. and G.R. characterized the rat insulinoma cell-line; M.I.M.,
896 A.L.G., T.T. and L.G. supervised the project; O.P.D., M.L., B.H., S.K., N.K., P.R., A.L.G., T.T.,
897 and L.G. wrote the manuscript; all authors revised the manuscript.

898

899

900 **Materials & Correspondence**

901 Correspondence and requests for materials should be addressed to L.G. (leif.groop@med.lu.se)
902 or A.L.G.(anna.gloyn@drl.ox.ac.uk)

903

904

905 **Competing interests**

906

907 L.G. has received research funding from Pfizer Inc, Regeneron Pharmaceuticals, Eli Lilly and Astra
908 Zeneca. N.L.B. and M.vD.B are now employees of Novo Nordisk, although all experimental work
909 was carried out under employment at the University of Oxford. ALG has received honoraria from
910 Novo Nordisk. MIM serves on advisory panels for Pfizer, Novo Nordisk, Zoe Global; has received
911 honoraria from Pfizer, Novo Nordisk and Eli Lilly; has stock options in Zoe Global; has received
912 research funding from Abbvie, Astra Zeneca, Boehringer Ingelheim, Eli Lilly, Janssen, Merck,
913 Novo Nordisk, Pfizer, Roche, Sanofi Aventis, Servier, Takeda.

914

915

916

917

918
919
920
921
922
923
924
925
926
927
928
929
930
931
932
933
934
935
936
937
938
939
940
941
942
943
944
945
946
947

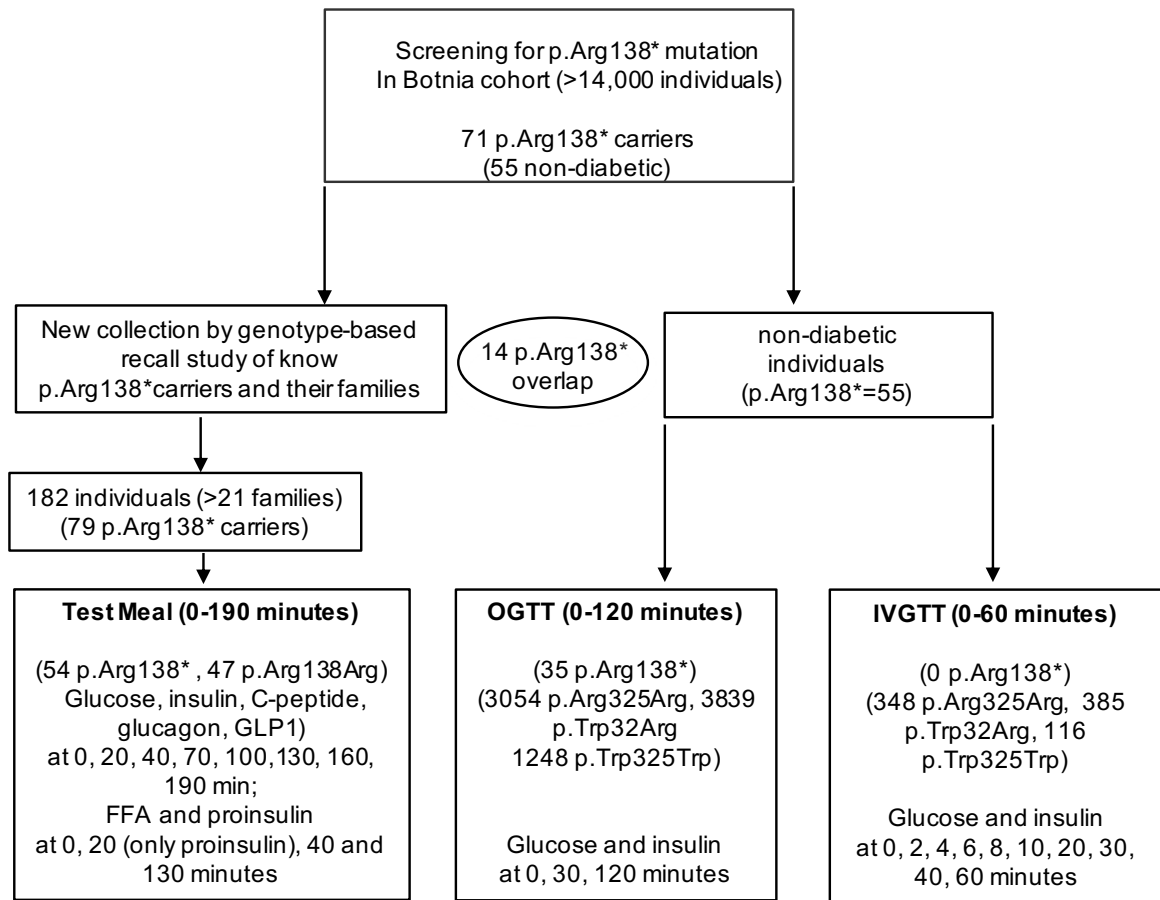
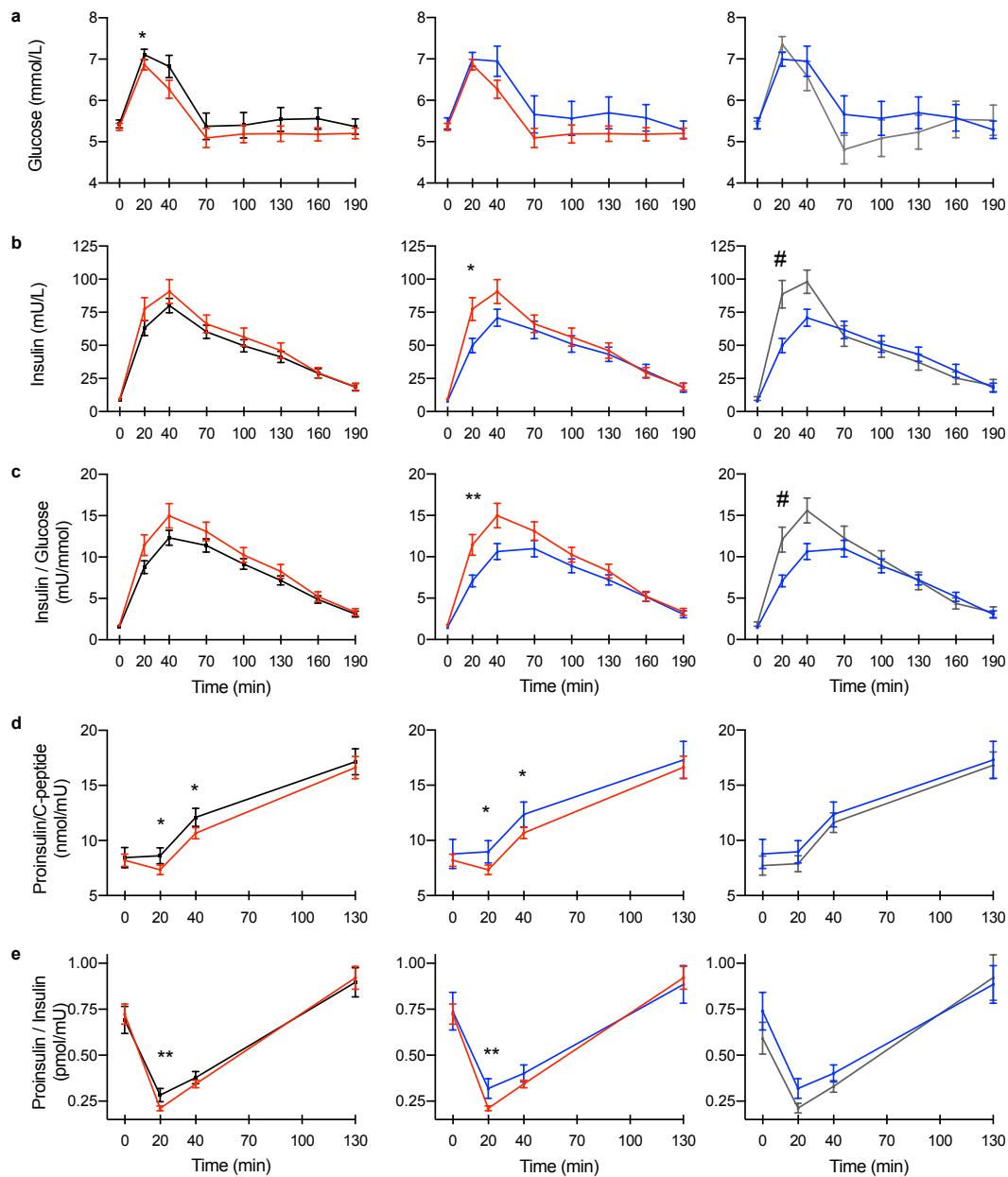


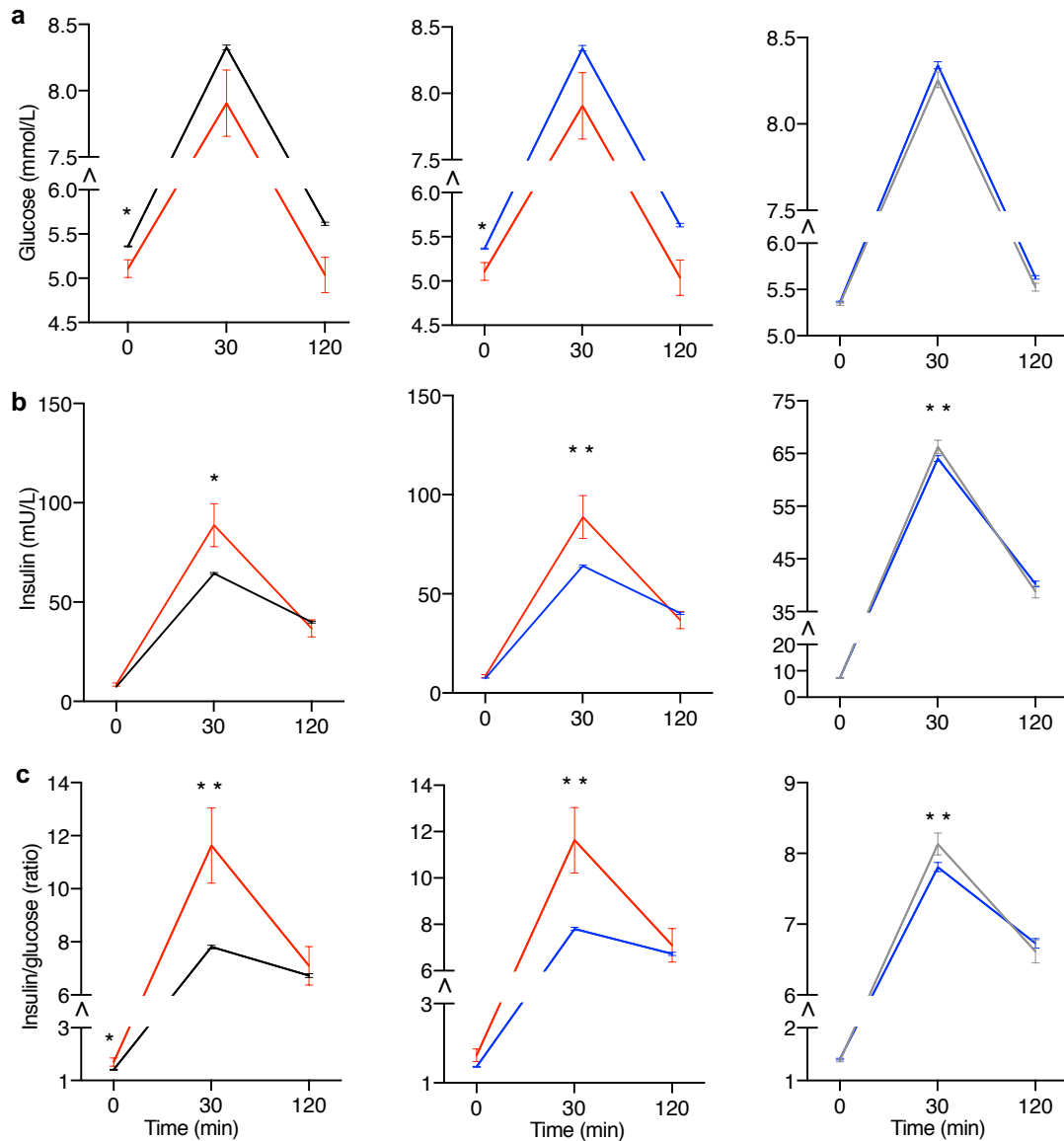
Fig. 1: A flow-chart of study design for human *in vivo* studies

948



949 **Fig. 2: SLC30A8-p.Arg138* enhances insulin secretion and proinsulin processing during test meal.**
 950 Association of *SLC30A8* p.Arg138* and p.Trp325Arg variants with **a**, plasma glucose **b**, serum insulin **c**,
 951 insulin/glucose ratio **d**, proinsulin/C-peptide ratio and **e**, proinsulin/insulin ratio during test meal. *Left panel*: Carriers
 952 (red, N=54) vs. non-carriers (black, N=47) of p.Arg138*. *Middle panel*: Carriers of p.Arg138* (red, N=54) vs
 953 Arg138Arg having the common risk variant p.Arg325 (blue, N=31). *Right panel*: Carriers of p.Trp325Trp (grey, N=16)
 954 vs. p.Arg325 (blue, N=31). Data are Mean \pm SEM. P-values were calculated by family-based association (*) or linear
 955 regression (#) (adjusted for age, sex, BMI and p.Trp325Arg variant status for the middle pane, Methods): */#, $p < 0.05$,
 956 **/##, $p < 0.01$.
 957

958
959
960
961
962
963
964
965
966
967
968
969
970
971
972
973
974
975
976
977
978
979
980
981
982



983
984
985
986
987
988
989
990
991
992
993
994

Fig. 3: *SLC30A8* p.Arg138* and p.Trp325 enhance insulin secretion during OGTT.

Association of *SLC30A8* p.Arg138* and p.Trp325Arg with **a**, plasma glucose **b**, serum insulin **c**, insulin/glucose ratio during an oral glucose tolerance test (OGTT). *Left panel*: Carriers (red, N=35) vs. non-carriers (black, N=7954-8141) of p.Arg138*. *Middle panel*: Carriers of p.Arg138* (red, N=35) vs. p.Arg138Arg having the common risk variant p.Arg325 (blue, N=6728-6893). *Right panel*: Carriers of p.Trp325Trp (grey N=1226-1248) vs. p.Arg325 (blue, N=6728-6893). Data are shown as Mean \pm SEM. P-values (mixed model, Methods) using additive effect: * < 0.05, ** < 0.01. Y-axis: note truncation (^) and different scale in the right panel.

995
996
997
998
999
1000
1001
1002
1003
1004
1005
1006
1007
1008
1009
1010
1011
1012
1013
1014
1015
1016
1017
1018
1019
1020
1021
1022
1023
1024
1025
1026
1027
1028
1029
1030
1031
1032

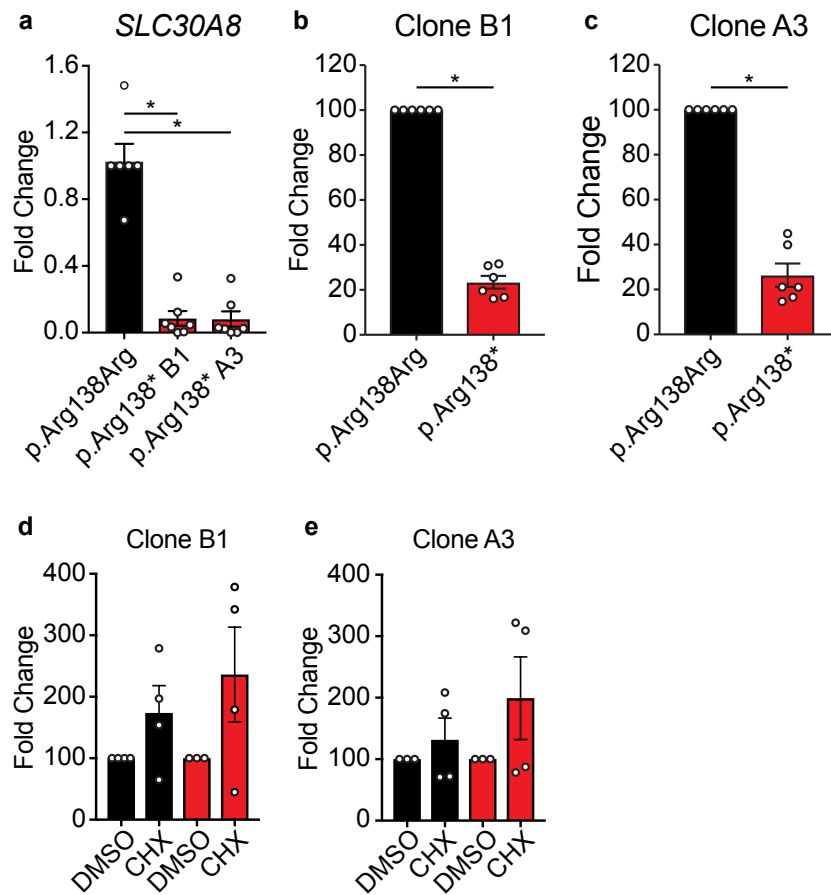


Fig. 4: Beta like cells derived from *SLC30A8*-p.Arg138* iPSCs display haploinsufficiency of *SLC30A8*.

a, *SLC30A8* expression in cells heterozygous for *SLC30A8*-p.Arg138*. Data normalized to *TBP* gene are expressed as fold change relative to p.Arg138Arg control (n=6-7 wells from two differentiations). Allele-specific expression (ASE) of p.Arg138Arg (black bar) and p.Arg138* (red bar) in **b**, clone B1 or **c**, clone A3 derived cells. Allele-specific expression of p.Arg138Arg (black bar) and p.Arg138* (red bar) in **d**, clone B1 and **e**, clone A3 derived cells treated with DMSO (Dimethyl sulfoxide) or cycloheximide (CHX) for four hours. ASE data (Mean \pm SEM) were determined by Digital Droplet PCR and presented as fold change relative to p.Arg138Arg transcript (**b**, **c**, n=6 wells from two differentiations) or to DMSO control (**d-e**, n=3-4 wells from two differentiation). * P<0.05 (Kruskal-Wallis test for multiple comparisons or unequal variance t-test).

1033
1034
1035
1036
1037
1038
1039
1040
1041
1042
1043
1044
1045
1046
1047
1048
1049
1050
1051
1052
1053
1054
1055
1056
1057
1058
1059
1060

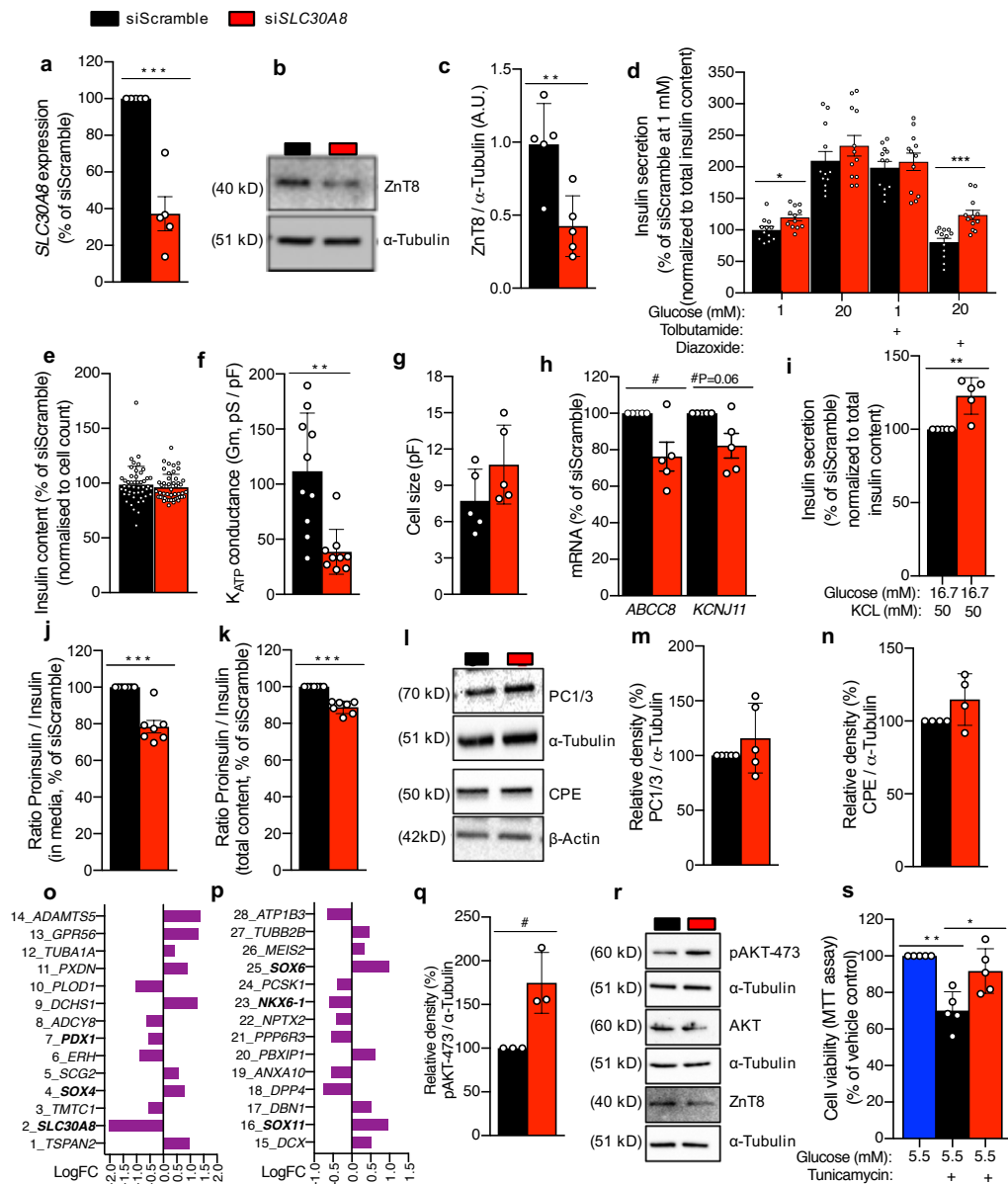


Fig. 5: *SLC30A8* knock down leads to enhanced insulin secretion, proinsulin processing and cell viability in the human pancreatic EndoC-βh1 cells.

a-c, Characterization of *SLC30A8* knock down (KD) at the (a) mRNA and protein level (b-immunoblot, c-densitometry). **d-i,** Effect of KD on (d) insulin secretion stimulated by glucose and K_{ATP} channel regulators (as labelled), (e) insulin content, (f) K_{ATP} channel conductance (Gm), (g) cell size, (h) expression of K_{ATP} channel subunits, (i) insulin secretion stimulated by KCL and high glucose. **j-n,** Effect of KD on proinsulin processing estimated by (j-k) proinsulin/insulin ratio and proinsulin processing enzymes PC1/3 and CPE (l, immunoblot, m-n, densitometry). **o-p,** Effect of KD (n=3 vs. 3) on whole transcriptome (mRNAs) by next generation sequencing and depicting 28 top candidate genes ranked by increasing p values (1% FDR corrected, P ≤ 0.0002). **q-s,** Effect of KD on basal (5.5 mM glucose) AKT phosphorylation (q, densitometry, r, immunoblot; phospho-AKT-Ser473, total AKT) and cell viability under ER stress (s, MTT assay, 10 μg/ml tunicamycin, DMSO as vehicle control). Data are shown as Mean ± SEM (N=3-10). P-values (*Mann-Whitney test/#Unpaired t test): */# p ≤ 0.05, ** p < 0.01, *** p < 0.001.

1073
1074
1075
1076
1077
1078
1079
1080
1081
1082
1083
1084
1085
1086
1087
1088
1089
1090
1091
1092
1093
1094
1095
1096
1097
1098

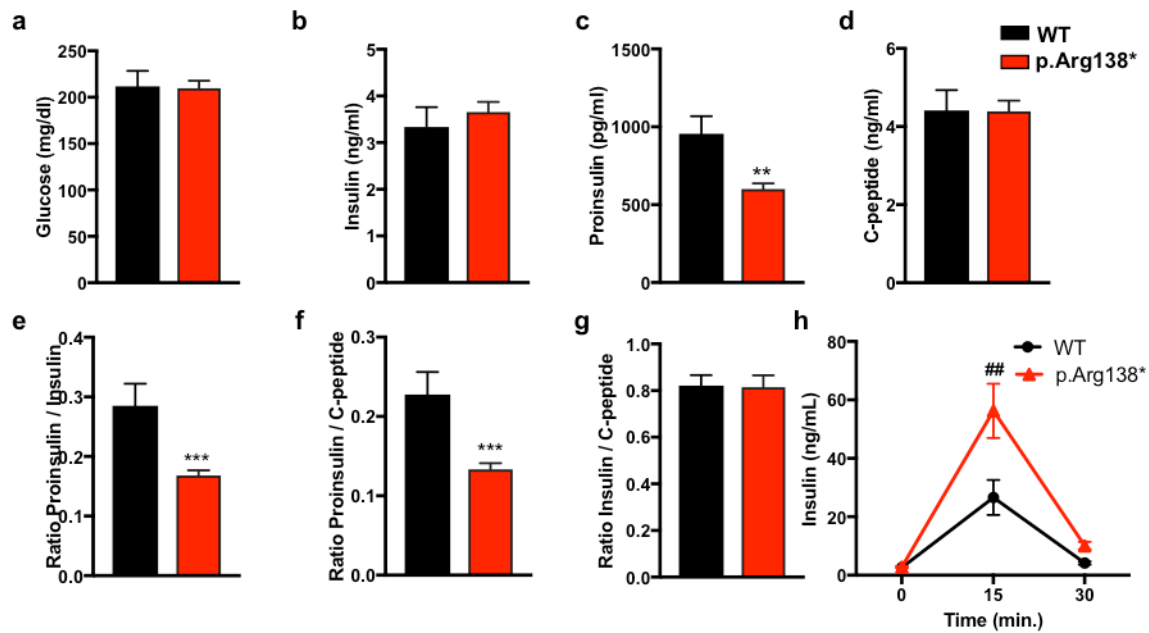
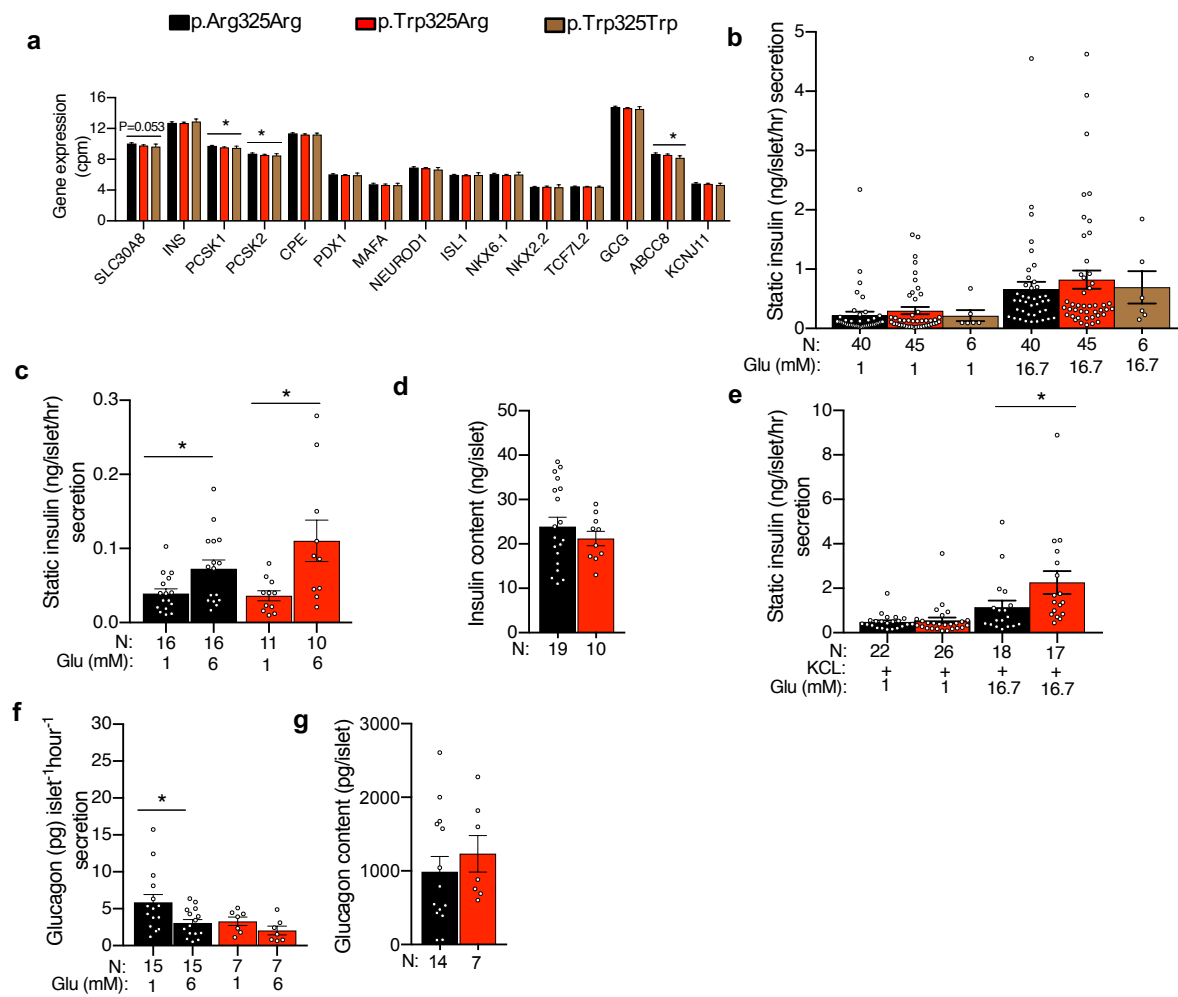


Fig. 6: Male p.Arg138* mice on high-fat diet show enhanced insulin secretion and proinsulin processing.

Circulating **a**, glucose **b**, insulin **c**, proinsulin **d**, C-peptide **e**, proinsulin/insulin ratio **f**, proinsulin/C-peptide ratio and **g**, insulin/C-peptide ratio in fasted WT and p.Arg138* mice (n= 10 WT, 17 p.Arg138*) after 20 weeks on HFD. **h**, Insulin response to oral glucose (2g/kg) exposure (n=5 WT, 11 p.Arg138*) after 30 weeks on HFD. p**<0.01, p***<0.005 using Students T test; p##<0.01 using two-way Anova.

1099



1100

1101 **Fig. 7: *SLC30A8*- p.Trp325 leads to enhanced insulin secretion in human islets.**

1102 **a**, Effect of p.Trp325Arg genotype (p.Arg325Arg=66, p.Trp325Arg=63 and p.Trp325Trp=11) on expression of
 1103 *SLC30A8* and other genes involved in insulin production, secretion and processing. **b**, Effect of p.Trp325Arg genotype
 1104 on static insulin secretion in presence of low and high glucose stimulatory conditions. **c-d**, Effect of p.Trp325Arg
 1105 genotype on static insulin secretion in **(c)** low stimulatory conditions and their **(d)** insulin contents. **e**, Effect of
 1106 p.Trp325Arg genotype on static insulin secretion in presence of low and high glucose and KCL. **f**, Static glucagon
 1107 response to glucose and **g**, glucagon content at basal glucose. Data are Mean \pm SEM; Glu- glucose. Analysis by linear
 1108 regression or Mann-Whitney test (Methods); * $p<0.05$.

1109

1110

1111

1112